



**TURUN
YLIOPISTO**
UNIVERSITY
OF TURKU

PHAGE-BIOSENSORS FOR DETECTION OF CANCER FROM URINE

Vilhelmiina Juusti



**TURUN
YLIOPISTO**
UNIVERSITY
OF TURKU

PHAGE-BIOSENSORS FOR DETECTION OF CANCER FROM URINE

Vilhelmiina Juusti

University of Turku

Faculty of Medicine
Institute of Biomedicine
Medical Physics and Engineering
Turku Doctoral Programme of Molecular Medicine (TuDMM)

Supervised by

Professor Pekka Hänninen Medical Physics and Engineering, Faculty of Medicine, University of Turku, Turku, Finland	PhD Janne Kulpakko Chief Scientific Officer, Aqsens Health Ltd., Turku, Finland
---	---

Reviewed by

Professor emeritus Mikael Skurnik Department of Bacteriology and Immunology, Faculty of Medicine, University of Helsinki, Helsinki, Finland	Professor Caglar Elbuken Faculty of Biochemistry and Molecular Medicine, Faculty of Medicine, University of Oulu, Oulu, Finland
--	--

Opponent

Professor Jouko Peltonen
Laboratory of Physical Chemistry,
Åbo Akademi University, Turku, Finland

The originality of this publication has been checked in accordance with the University of Turku quality assurance system using the Turnitin OriginalityCheck service.

Cover Image: Sylvia and Vilhelmiina Juusti

ISBN 978-952-02-0009-1 (PRINT)
ISBN 978-952-02-0010-7 (PDF)
ISSN 0355-9483 (Print)
ISSN 2343-3213 (Online)
Painosalama, Turku, Finland 2025

Vanhemmilleni

UNIVERSITY OF TURKU

Faculty of Medicine

Institute of Biomedicine

Medical Physics and Engineering

VILHELMIINA JUUSTI: Phage-biosensors for urine-based cancer detection

Doctoral Dissertation, 122 pp.

Turku Doctoral Programme of Molecular Medicine

January 2025

ABSTRACT

Detection and classification of cancer is challenging because current methods are often clinically ambiguous, expensive and/or laborious. Molecular tests have been developed over past decades but they lack accuracy, clinical applicability and are poorly scalable to population level screening. New methods are needed to meet the requirements of modern healthcare and to overcome challenges of cancer detection. Non-invasive sampling together with a novel detection method could enable affordable and scalable cancer detection.

In this work, phage-biosensors were developed to detect specific biomarkers and cancer from non-invasive urine samples. Phages can be used as bioreceptors in modern biosensors. They are robust, affordable, easily modifiable, and quick to produce in large amounts. In cancer detection, they were combined with chemical modulation of time-resolved fluorescence to enhance the detection sensitivity and accuracy. Phages were selected in a two-stage affinity selection and used in biosensors. Results were measured via optical detection with both time-resolved fluorescence and absorbance. Biosensors were developed towards model analytes and different cancers from urine. The biophysical properties of the biosensor method were studied with biomarkers to understand behaviour in the detection reaction.

Phage-biosensors detected lethal prostate cancer with sensitivity of 80% and specificity of 75% and metastatic cancer respectively with 70% sensitivity and 79% specificity. An infection indicator C-reactive protein (CRP) was detected at a clinically relevant area. Liquid Crystalline behaviour of the biosensor was studied in detection of Green Fluorescent Protein (GFP) with the limit of detection was 0.24 $\mu\text{g/ml}$.

The method is suitable for analyzing non-invasive samples, such as urine, and single biomarkers. The method may offer novel ways to detect cancer and target multiple biomarkers at once from non-invasive samples.

KEYWORDS: phage, biosensor, cancer, cancer detection, urine, non-invasive

TURUN YLIOPISTO

Lääketieteellinen tiedekunta

Biolääketieteen laitos

Lääketieteellinen fysiikka ja tekniikka

VILHELMIINA JUUSTI: Faagibiosensoreita virtsapohjaiseen syövän havaitsemiseen

Väitöskirja, 122 s.

Molekyyllilääketieteen tohtoriohjelma

Tammikuu 2025

TIIVISTELMÄ

Syövän havaitseminen ja luokittelu on haastavaa nyky menetelmillä, koska ne ovat ovat kalliita ja/tai työläitä ja tulokset ovat kliinisesti epäselviä. Molekulaarisia testejä on kehitetty vuosikymmeniä, mutta ne ovat epätarkkoja ja puutteellisia kliininen sovellettavuuden ja populaatiotason skaalattavuuden osalta. Tarvitaan uusia modernin terveydenhuollon vaatimuksia vastaavia menetelmiä, jotta voidaan ratkaista syövän havaitsemiseen liittyvät haasteet. Noninvasiiviset näytteet yhdessä uudenlaisten ilmaisumenetelmien kanssa voivat olla ratkaisu näihin haasteisiin. Bakteriofageja eli faageja käytetään bioreseptoreina moderneissa biosensoreissa ja ne ovat kestäviä, edullisia, helposti muokattavissa olevia sekä nopeita tuottaa suurissa määrissä.

Tässä työssä faagibiosensoreita kehitettiin havaitsemaan tiettyjä biomerkkiaineita sekä syöpää noninvasiivisista näytteistä. Syövän havaitsemisessa ne yhdistettiin aikaerotteisen fluoresenssin kemialliseen modulaatioon mittausten herkkyyden sekä tarkkuuden parantamiseksi. Biosensoreissa käytetyt faagit valittiin kaksivaiheisen affiniteettivalinnan kautta ja tulokset mitattiin optisilla havaitsemistekniikoilla eli aikaerotteisella fluoresenssilla ja absorbanssilla. Biosensorit kehitettiin mallimerkkiaineiden sekä syövän merkkiaineiden havaitsemiseen virtsanäytteistä. Biosensorin biofysikaalisia ominaisuuksia tutkittiin mallimerkkiaine GFP:n kanssa havaitsemisreaktion taustalla olevien biofysikaalisten ilmiöiden selvittämiseksi.

Faagibiosensorit havaitsivat tappavan eturauhassyövän 80% herkkyydellä ja 75% tarkkuudella, ja vastaavasti metastaatista syövän 70% herkkyydellä ja 79% tarkkuudella. Infektiomerkkiaine C-reaktiivinen proteiini (CRP) havaittiin kliinisesti merkittäväällä tasolla. Nestekidekäyttäytyminen todennettiin havaitsemalla vihreää fluoresoivaa proteiinia (GFP) (havaitsemisraja 0.24 µg/ml).

Menetelmä sopii noninvasiivisten virtsanäytteiden ja yksittäisten biomerkkiaineiden analysoimiseen. Menetelmä voi tarjota uuden tavan havaita syöpä ja useita biomerkkiaineita samanaikaisesti noninvasiivisista näytteistä.

AVAINSANAT: faagi, biosensori, syöpä, syövän havaitseminen, virtsa, noninvasiivinen

Table of Contents

Abbreviations	8
List of Original Publications	10
1 Introduction	11
2 Review of the Literature	13
2.1 Optical measurement methods.....	13
2.1.1 Luminescence	13
2.1.2 Colorimetry.....	15
2.1.3 Interferometry.....	15
2.2 Phages.....	16
2.2.1 Morphology and genome of M13.....	18
2.2.2 Life cycle.....	19
2.2.3 Liquid crystalline behaviour	21
2.2.4 Modification techniques.....	22
2.2.4.1 Genetic engineering methods	22
2.2.4.2 Chemical modification.....	25
2.3 Biosensors	26
2.3.1 General structure	26
2.3.2 Advantages and possibilities	27
2.3.3 Optical biosensors.....	27
2.3.4 Phage-biosensors	28
2.3.4.1 Optical phage-biosensors	29
2.3.4.1.1 Luminescent biosensors.....	29
2.3.4.1.2 Colorimetric biosensors.....	30
2.3.4.2 Phage-biosensor applications in cancer detection.....	31
2.4 Cancer	32
2.4.1 Hallmarks of cancer	32
2.4.2 Urological cancers.....	33
2.4.3 Clinical detection of cancer	35
2.4.3.1 Imaging.....	35
2.4.3.2 Biopsy.....	36
2.4.3.3 Molecular analysis	36
2.4.4 Prospects in cancer detection	37
3 Aims	40

4	Materials and Methods	41
4.1	Phages and microbes.....	41
4.2	Other biosensor components	41
4.3	Model biomarkers.....	42
4.4	Clinical samples	42
4.5	Optical measurement methods.....	43
4.6	Biopanning procedures	43
	4.6.1 Coating with the target.....	44
	4.6.2 Affinity selection of phages.....	44
4.7	Biosensor assays	45
4.8	Functioning principle of the biosensor	46
4.9	Chemical assay for cancer detection.....	47
4.10	Data analysis.....	47
5	Results	49
5.1	Demonstration with model biomarker and screening lethal prostate cancer (I).....	49
	5.1.1 Detection of model biomarker CRP	49
	5.1.2 Screen of lethal prostate cancer	50
5.2	Biophysical properties of detection phenomena in phage-biosensor (II).....	51
	5.2.1 Quantitative detection of GFP with optical methods.....	51
	5.2.2 Lyotropic properties of phage-biosensor.....	55
	5.2.3 Thermotropic properties of phage-biosensor	56
5.3	Improved biopanning protocol and classification of metastatic cancer (III).....	57
	5.3.1 Major changes in methods	57
	5.3.2 Chemical sensor for cancer	57
	5.3.3 Phage-biosensor for metastatic cancer	58
6	Discussion	61
6.1	Clinical samples	61
6.2	Biopanning	61
6.3	Biosensor assays	63
	6.3.1 Detection of model analytes	63
	6.3.2 Biosensor-based detection of PCa and metastases	64
6.4	Liquid crystalline properties of phage-biosensor.....	66
6.5	Chemical sensor	67
6.6	Data analysis.....	67
6.7	Clinical impact and future perspectives	68
7	Conclusions	71
	Acknowledgements	72
	References	74
	Original Publications	85

Abbreviations

AA	Amino acid
AUC	Area under curve
BCa	Bladder cancer
cfDNA	Cell-free DNA
CRISPR/Cas9	The clustered regularly interspaced short palindromicrepeats (CRISPR)-CRISPR-associated protein 9 (Cas9) system
CRP	C-Reactive Protein
CT	Computed tomography
ctDNA	Circulating tumor DNA
cv	Coefficient of Variation
ds	Double-stranded
EIA	Enzyme immunoassay
EIS	Electrochemical impedimetric spectroscopy
ELISA	Enzyme linked immunosorbent assay
FDG	Fluorodeoxyglucose
FRET	Förster resonance energy transfer
GFP	Green Fluorescent Protein
GG	Gleason Group
gRNA	GuideRNA
HDR	Homology-directed repair
HPV	Human papillomavirus
HR	Homologous Recombination
KCa	Kidney cancer
LC	Liquid crystalline
LC-MS	Liquid chromatography-mass spectrometry
LoD	Limit of Detection
mCa	Metastatic cancer
MCP	Major capsid protein
miRNA	MicroRNA
MRI	Magnetic Resonance Imaging
mRNA	MessengerRNA

NHEJ	Non-homologous end-joining
NMR	Nuclear magnetic resonance
NTA	1-(2-Naphthoyl)-3,3,3-trifluoroacetone
PCa	Prostate cancer
PET	Positron emission tomography
PoC	Point-of-Care
PSA	Prostate specific antigen
PSMA	Prostate-specific membrane antigen
RDT	Rapid diagnostic test
RF DNA	Replicative form of dsDNA
ROC	Receiver operating characteristic
RT	Room temperature
SEM	Standard error of mean
SERS	Surface enhanced Raman scattering
SPR	Surface plasmon resonance
ss	Single-stranded
TCC	Transitional cell carcinoma
TOPO	Trioctylphosphine oxide
TRF	Time-resolved fluorescence
UC	Urothelial carcinoma
VEGF	Vascular endothelial growth factor
VOCs	Volatile organic compounds
WHO	World Health Organization

List of Original Publications

This dissertation is based on the following original publications, which are referred to in the text by their Roman numerals:

- I Kulpakko Janne, **Juusti Vilhelmiina**, Rannikko Antti, Hänninen Pekka. Detecting disease associated biomarkers by luminescence modulating phages. *Scientific Reports*, 2022; 12: 2433. This original publication has already been included in the thesis book of PhD Janne Kulpakko in year 2022.
- II **Juusti Vilhelmiina**, Kulpakko Janne, Cudjoe Elizabeth, Pimenoff Ville N., Hänninen Pekka. Biophysical Properties of Bifunctional Phage-Biosensor. *Viruses*, 2023; 15: 299.
- III **Juusti Vilhelmiina**, Rannikko Antti, Laurila Anu, Sundvall Maria, Hänninen Pekka, Kulpakko Janne. Phage-biosensor for classification of metastatic urological cancers from urine. *Life*, 2024; 14: 600.

The original publications have been reproduced with the permission of the copyright holders.

1 Introduction

Cancer is a complex systemic disease causing millions of deaths all over the World annually. Even though cancer has plagued humans from ancient times and the importance of early detection and removal for prognosis has been recognized since then (Hajdu, 2011), modern medicine is still struggling to overcome cancer despite the efforts of centuries. Especially, aggressive and advanced metastasized cancers are often detected late. This troubles the treatment and prognosis, and causes ~ 90% of cancer-related deaths (Connal et al., 2023). Current screening, detection and diagnostic methods, such as biopsies, imaging and molecular tests, fail often in sensitivity and can usually detect cancer once it has developed into a carcinogenic form (Wu et al., 2022).

New methods are urgently needed to detect cancer early as possible in routine check-up (Bax et al., 2019; Pal et al., 2022). They should meet the clinical needs of being highly sensitive, specific, affordable, quick, pleasant for both patients and users, and environmentally friendly. In addition, new methods could enable discovery of new cancer-related biomarkers and multiplexing several biomarkers to one test that could improve not only diagnostics, but prognosis, treatment and follow-up (Kumar et al., 2023; Pal et al., 2022). These biomarkers can be identified from liquid biopsies rich of various biomolecules. For example, urine is an interesting option due to its non-invasiveness, safety and easy access (Pal et al., 2022).

New biosensor methods are an attractive option for conventional molecular tests detecting cancer-related biomarkers (Elois et al., 2023). Optical biosensors, particularly with fluorescent and colorimetric transducers, are a competitive alternative when compared to other physical biosensors because of their applicability to biomedical testing, high sensitivity, robustness to external factors, and low noise (Chen & Wang, 2020; Kamel & Khattab, 2020; Kim et al., 2016). A biosensor needs a bioreceptor with high affinity towards the target biomarker. Various biomolecules have been used as bioreceptors in biosensors, such as antibodies, cells and nucleic acids (Naresh & Lee, 2021). However, they may lack some of the needed properties in regards of sensitivity, robustness, cost, applicability, and production (Bhalla et al., 2016).

Phages are viruses that infect bacteria (Hay & Lithgow, 2019) which have had a major effect on biotechnology since their discovery in the early 1900s (Carmody et al., 2021). They can be used as bioreceptors in modern biosensors and analytical platforms (Ahovan et al., 2020) and meet the needed requirements of biomarker detection (Brödel et al., 2018; Yang et al., 2013). They can be engineered and modified with multiple methods (Alfaleh et al., 2020; Carmody et al., 2021; Chung et al., 2014), and their self-assembly and liquid crystalline (LC) properties (Sawada, 2017; Secor et al., 2015; Yang et al., 2013) can be utilized in fluorescent and colorimetric biosensors (Rakonjac et al., 2023; Sawada & Serizawa, 2018; Yang et al., 2013). Phage-biosensors offer a tempting opportunity to develop biosensors for cancer detection to surpass the current screening and detection methods.

The main focus of this thesis was phage-biosensors and their applications in urine-based cancer detection. Results are reported herein from developing protocol to demonstrating their usability in single analyte detection, and applying them to screen aggressive prostate cancer (PCa) and detecting metastatic cancer (mCa). Additionally, their biophysical properties were studied to explain phenomena in the detection interactions between the phages and target biomarkers.

2 Review of the Literature

This review of literature provides the scientific background for the experimental section of this dissertation. Topics are focused primarily on a few optical measurement methods, phages, and their use in modern biosensors. In addition, cancer as a disease is introduced at a general level.

2.1 Optical measurement methods

Optical measurement methods use light to measure the various properties of an object without contact. They can be used to measure molecular composition or interactions, for example.

2.1.1 Luminescence

Luminescence is a phenomenon where any substance emits light from electronically or vibrationally excited states (Bolton, 1996; Lakowicz, 2006). Formally luminescence is divided into two categories depending on the excited state: 1) fluorescence and 2) phosphorescence. In fluorescence, when a molecule absorbs light, it is excited to a higher vibrational level. Then it returns spontaneously to ground state and emits a photon detected as a fluorescence. However, molecules can go through a spin conversion to the first triplet state (intersystem crossing) and emission from that state is called phosphorescence. Phosphorescence emission generally has longer wavelengths and lower energy than fluorescence (Lakowicz, 2006). These transitions between different molecular states are presented as a simple Jablonski diagram in Figure 1.

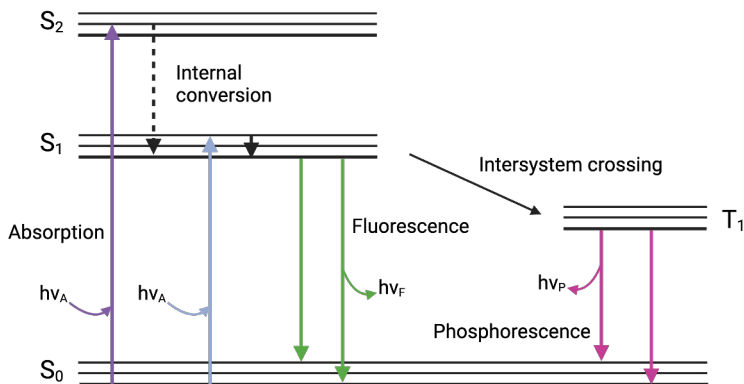


Figure 1. Simplified Jablonski diagram presenting molecular transits during excitation and emission of a molecule. The singlet ground, first, and second electronic states are portrayed with S₀, S₁ and S₂. The first triplet state is portrayed with T₁. In excitation, radiation is absorbed ($h\nu_A$) and electrons transit to upper states. In emission, radiation is released via either fluorescence ($h\nu_F$) or phosphorescence ($h\nu_P$) when an electron transits back to the ground state. Modified from Lakowicz (Lakowicz, 2006). Figure created with BioRender.com.

In addition, luminescence can be classified based on the source of luminescence excitation, such as bioluminescence, chemiluminescence and electroluminescence. Bioluminescence is emitted by living organisms, such as cells, and chemiluminescence and electroluminescence respectively by chemiexcitation and electrode reactions (Bolton, 1996). Time-resolved fluorescence (TRF) is special fluorescence with long lifetime (milliseconds) displayed by lanthanides, such as europium, terbium and ytterbium. This special feature of lanthanides is based on electronic transitions between shielded orbitals, and low emission rates by their small extinction coefficients. TRF emission can be measured after the autofluorescence from biological samples has decayed. Short-lived autofluorescence lasts nanoseconds and causes background signal and often hinders the sensitivity of detection. Emission of TRF after the disappearance of autofluorescence makes lanthanide-based systems more sensitive than systems using conventional fluorophores (Lakowicz, 2006).

Different types of luminescence are widely used for detection in biomedical assays, bioimaging and beyond. The most known bioassays are enzyme immunoassay (EIA), and enzyme linked immunosorbent assay (ELISA). EIA was developed in the 1960s and ELISA right after in early the 1970s. Basically they have the same working principles. Still today, they are used worldwide in analytical and clinical studies and routine patient screening. The end-product of ELISA is quantified with colorimetric, fluorescent, or luminescent measurement (Hosseini et al., 2018). Molecules emitting fluorescence and phosphorescence also have been widely used in bioimaging, biosensing (Feng et al., 2023) and immunoassays (Diamandis, 1988) already for

decades. Recently modern approaches have been developed. For example, Khan *et al.* used a highly sensitive nanoparticle-aided TRF immunoassay to detect renal cell carcinoma based on extracellular vesicles (Khan *et al.*, 2024).

2.1.2 Colorimetry

Colorimetry quantitatively describes a colour. Absorbance, known as optical density, is the quantity of light absorbed by a solution. More detailed, it is the base-10 logarithm of the ratio between the spectral radiant power of the light incident on the sample (P^0) and the spectral radiant power of the light transmitted through the sample (P^1) (equation 1) (Bolton, 1996).

Equation 1. Formula for absorbance.

$$A = \log(P_{\lambda}^0/P_{\lambda}^1) = -\log T$$

Absorbance is widely used in biomedicine from basic research to many modern applications. The primary mechanism is structural color changes that appear during the detection at nanometer-scale (Kinoshita & Yoshioka, 2005; Lee *et al.*, 2021). One simple application used for decades is determining protein concentration in urine (Savory *et al.*, 1968). Many potential biomedical applications utilizing absorbance have been developed over the years. Such as, Takiwaki *et al.* used absorbance spectra analysis to detect pathophysiological changes in skin lesions (Takiwaki *et al.*, 2004) and Xu *et al.* developed absorbance-based colorimetric aptasensor for detecting cancer-derived exosomes (Xu *et al.*, 2020).

2.1.3 Interferometry

Interferometry measures quantitatively interference of waves. The refractive index (n) determines the speed of light travelling through a medium. In interferometry, the measurement involves observing the reference beam, and the sample, which is influenced by the measurement beam. When the refractive index varies within the sample, the interference signal is attenuated or amplified accordingly. Interference is an extremely sensitive measurement technique. The light can travel with the speed of light (c) only in vacuum because electromagnetic waves do not experience dispersion in such condition. The speed of light slows down in other materials (c_n). Refractive index may be affected by many parameters, such as the wavelength, energy, direction of propagation, state of polarization of a ray of light, temperature, density and scattering of light in solids. In practice, the refractive index is the angle between reflected and refracted light through different materials (Gallegos & Stokkermans, 2023).

Equation 2. Formula for refractive index.

$$n = \frac{c}{c_n}, c = 299\,792\,458 \frac{m}{s}$$

Monitoring of refractive index has many clinical applications due to connection to optical properties of materials, such as biological tissues and liquids. Refractive index measurements from basic research to industrial applications in biomedicine have been lately reviewed (Khan et al., 2021). To highlight, refractive index is used as a key parameter in studying biophysics of biological materials. It correlates with mechanical, electrical and optical properties and provides information for different biological models. Optical sensors have been developed based on refractive index to detect and measure different targets. Parvin *et al.* developed a sensor detecting cancerous cells in human cervix, adrenal gland, breast, skin, and blood (Parvin et al., 2021). Ansari *et al.* measured haemoglobin concentration in human blood samples (Ansari et al., 2023), and Wang *et al.* combined surface plasmon resonance (SPR) chip to create a refractive index array to detect protein in human urine (Wang et al., 2022).

2.2 Phages

Phages are viruses infecting bacteria, and their variety is endless regarding morphology, genome size, structure and sequences. Globally they are the dominant biological entity, and constantly growing genome and metagenome sequence data testifies their diversity and huge impact on life on the Earth (Hay & Lithgow, 2019).

Shortly, their genome can consist of either double-stranded (ds) or single-stranded (ss) DNA or RNA. The genetic material is packaged inside a capsid that may have a polyhedral, filamentous, or pleomorphic shape, and may be connected to the tail. Their structure makes them stable in broad environmental conditions such as in different ranges of pHs, temperatures and dissolvents. Therefore, they are suitable for various practical applications (Rakonjac et al., 2023), like biomaterials (Sawada & Serizawa, 2018; Yang et al., 2013) and biorecognition elements in biosensors (Peltomaa et al., 2019). The taxonomy of bacterial viruses has recently shifted from a focus on morphology to a genome-based classification system. While morphological identifiers remain important, they no longer hold formal taxonomical significance. Altogether, there are 3601 different species of bacterial viruses in 47 families (Turner et al., 2023). Figure 2 presents different genomes and examples of morphological diversity of phages (Elbreki et al., 2014).

Phages can be classified to three main lineages based on lifestyle. Although these lineages are widely used, there is no universal consensus on them (Valencia-

Toxqui & Ramsey, 2024). These categories are briefly outlined to highlight how the M13 phage differs from other bacterial viruses in terms of its infection cycle. Phages can have either 1) lytic or productive (*virulent phage*), 2) temperate or lysogenic (*temperate phage*) (Guttman et al., 2004; Peltomaa et al., 2016), or 3) chronic infection cycle (Valencia-Toxqui & Ramsey, 2024). Virulent phages multiply only through a lytic cycle where they infect the host cell by releasing their genome into it and taking over the host metabolism to produce progeny phages. After some min or hours, the host cell lyses and releases a large number of progeny phages. Temperate phages have two options for their reproduction. They may directly initiate the lytic cycle and cell lysis releasing progeny phages or they enter the lysogenic cycle where the phage genome does not replicate but is in a quiescent state as a prophage. The prophage resides in the host cell either integrated to the host genome or as a plasmid. The prophage stays in this state indefinitely by repressing the lytic cycle genes, and is replicated together with its host cell, making all host descendants to contain the prophage. The prophage may enter the lytic cycle when the host cell encounters adverse conditions and the SOS response of the host cell causes the degradation of the lytic cycle repressor (Guttman et al., 2004). Certain phages, such as M13, establish chronic infections in their host cells, releasing virions without causing cell death. The infection cycle of M13 will be described in more detail in chapter 2.2.2.

This chapter focuses on the “workhorse” of this thesis, M13 phage.

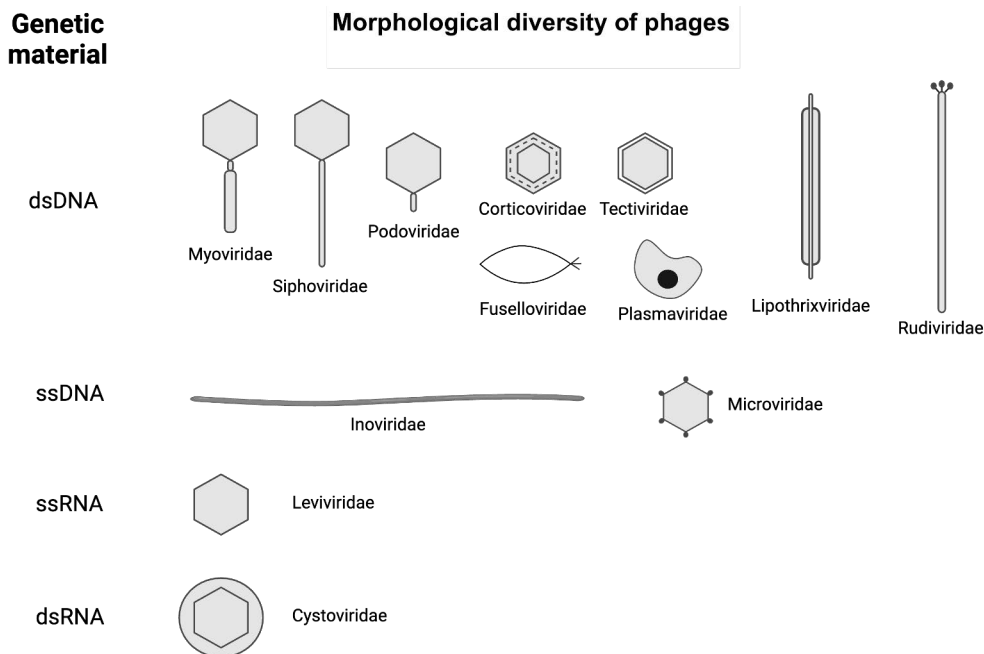


Figure 2. Genomes and morphological diversity of phages. The taxonomy of bacterial viruses has shifted from a focus on morphology to a genome-based classification system. While morphological identifiers remain important, they no longer hold formal taxonomical significance (Turner et al., 2023). Figure modified from Elbreki *et al.* (Elbreki et al., 2014). Figure created with BioRender.com.

2.2.1 Morphology and genome of M13

M13 is a non-lytic filamentous phage belonging to the family of *Inoviridae*. This family contains a large number of different phages whose morphology and lifestyle are exceedingly heterogeneous. Their genome consists of ssDNA and is packed to a long filament whose length is > 500 nm (Dion et al., 2020). The size of M13 is determined by its capsid proteins, and its length is ~ 800 nm and the diameter is ~ 6 nm (Wang et al., 2023). M13 displays compliance and enthalpic stretching, or simply linear elasticity instead of actual polymer extension. This makes them robust but adaptable structures (Khalil et al., 2007). M13 has a well-defined genome encoding 11 phage proteins (Wezenbeek et al., 1980). The genome is packed inside a capsid, which is formed by five types of capsid proteins: p3, p6, p7, p8, p9. P8 is the major capsid protein.

All p8s consist of three domains: 1) positively charged domain (40–50 AA) interacting electrostatically with genomic DNA of the phage, 2) intermediate hydrophobic domain (21–39 AA), and 3) *N*-terminal domain (1–20 AA). Phage DNA is helically wrapped within ~ 2700 copies of p8 protein via electrostatic interaction between ssDNA of the phage and positively charged domain. This causes negative charge on the phage surface. The large number of p8 copies forms $\sim 98\%$ of the whole

mass of M13. Rest of the capsid proteins are minor capsid proteins having 3–5 copies each. The minor coat proteins p3 and p6 are located on one end, and p7 and p9 on the other (Wang et al., 2023). Minor coat proteins primarily form the terminal parts of the phage capsid but p3 also has a significant role in recognition and infection of host cells and it is commonly used for the display of polypeptides (Smeal et al., 2017; Wang et al., 2023). Morphology of M13 is presented in Figure 3.

In addition to 5 coat proteins, M13 encodes 6 proteins needed for its replication. These are the regulatory and control proteins: p2, p5, p10, and the proteins forming the membrane spanning phage assembly complex: p1 (an inner membrane spanning protein), p4 (an outer membrane spanning protein), p11 (an inner membrane anchored periplasmic protein) (Haigh & Webster, 1999; Marciano et al., 1999; Russel, 1993).

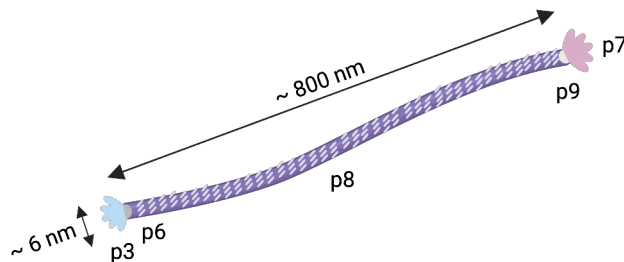


Figure 3. Morphology and capsid proteins of M13 phage. Adapted from Wang *et al.* (Wang et al., 2023). Figure created with BioRender.com.

2.2.2 Life cycle

Filamentous phages, like M13, are lysogenic. They do not lyse the host cell (Peltomaa et al., 2016). Their unique morphology and morphogenesis enable them to exit through the envelope of the host cell without killing it (Young et al., 2000).

The life cycle of M13 phage contains six steps (Ryu, 2017):

1. Attachment
2. Penetration into the host cell
3. Uncoating
4. Gene expression and replication
5. Assembly
6. Release

Early steps 1–3 are poorly understood but the entry of the phage genome is mediated by minor coat protein p3 interacting with the *F* pilus of *E. coli* (Bennett et

al., 2011). The genome is converted to dsDNA by combined action of host and phage. The replicative form of dsDNA (RF DNA) triggers messengerRNA (mRNA) transcription factors delivering mRNA for the synthesis of proteins encoded by the phage (step 4). The ss copies are converted into RF DNA that acts as a template for synthesizing additional ss copies of the M13 genome through rolling circle replication. This happens at early stages of step 4 when concentrations of phage proteins are still low. When concentrations of phage proteins, particularly p5 increase, the synthesization of RF DNA from ssDNA decreases because p5 binds to ssDNA copies and inhibits the conversion to RF DNA. In the step 5, the membrane spanning phage assembly complex recognizes p5 bound ssDNAs coated with p8s and pack the ssDNA to progeny phages (Haigh & Webster, 1999; Marciano et al., 1999; Russel, 1993). The assembly process is poorly understood. However, first the complex binds the minor coat protein p7 and p9 to the p5 bound ssDNA and then simultaneously ssDNA is transferred through the cell membranes. P5 is removed and p8 is bound around the phage genome. Finally, the minor coat proteins p3 and p6 are attached to the phage and a particle is released from the cell (step 6) (Bennett et al., 2011).

Detailed life cycle of M13 is presented in Figure 4 (Smeal et al., 2017).

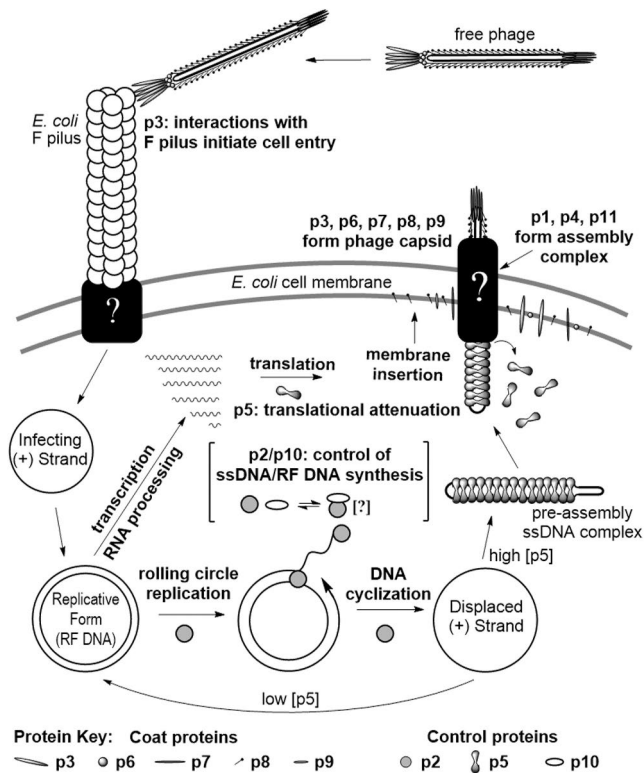


Figure 4. Detailed life cycle of M13 phage by Smeal et al. (Smeal et al., 2017).

2.2.3 Liquid crystalline behaviour

LC behaviour refers to the molecular ordering of biomolecules and cell membranes into specific patterns. This occurs in some biological processes and may also be due to self-assembly of molecules (Yang et al., 2013). Also filamentous M13 has a self-assembling nature. This is because of the well-known molecular properties of filamentous phages, such as their monodispersity, interparticle interactions, length and charge (Dogic & Fraden, 2000, 2006). These properties cause in suitable conditions equilibrium and non-equilibrium phase behaviour where phase transitions occur (Onsager, 1949). In colloidal suspensions, this leads to liquid crystal formation (Dogic & Fraden, 2000, 2006). Physically the phase behaviour is a consequence of the competition between rotational and translational entropy (Onsager, 1949) and, therefore makes these phages a usable model for studying physical properties of liquid crystals in practice. Virtually, these phages just spontaneously align and form liquid crystals due to steric forces between adjoining phages (Secor et al., 2015). Molecular interaction mechanisms between M13 and its targets occur with common functional groups. Strong adhesion energy may involve π - π stacking primarily with aromatic rings and hydrophobic forces with non-polar groups. Weaker interactions via hydrogen bonding occurs for example with carboxylic acids. In addition, external factors such as phage concentration, temperature, acidic environment and pH affects remarkably the interaction between phage and its targets (Lim et al., 2019). These factors also notably affect liquid crystal formation of M13. Thermotropic liquid crystals transit through different phases within a temperature range due to thermal movement of phage particles (Yang et al., 2013). They are formed via supramolecular interactions and fragile phage structures make dispersing them back to aqueous solutions impossible. They are prone to form nematic ordering because of their rigidity and grand length-to-diameter ratio (Liu et al., 2014).

However, lyotropic liquid crystals also are influenced by the temperature, but particularly by the concentration of phage particles. Their phases vary more than phases in thermotropic liquid crystals (Yang et al., 2013). The phases of M13-based lyotropic behaviour are isotropic, nematic, cholesteric and smetic (Sawada, 2017; Yang et al., 2013). Schematic structures of these phases with M13 are presented in Figure 5. At the isotropic phase, the concentration of phages is low and they are not organized at all. When phage amount is moderately increased, the distance between neighboring phages decreases. When the distance is less than the length of the phage, the phage particles assemble themselves to orientationally ordered configurations which is called nematic phase. When concentration continues to increase, phages start to entwine with each other. This occurs along the perpendicular axis of layers and causes a helicity of the phages. Then at some point, an increasing distinction in the helicity of the layers causes the transition to cholesteric phase. If increase in phage concentration is continued, phages are organized both positionally and

orientationally to well defined phases. This transition to the smectic phase happens only at very high phage concentrations. Smectic phase vary based on the degrees of positional and orientational order (Yang et al., 2013).

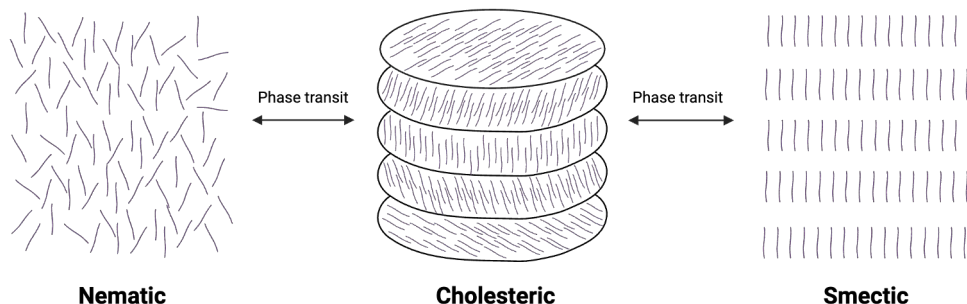


Figure 5. Schematic structures of the liquid crystalline (LC) phases of M13 phage. Modified from Yang *et al.* (Yang et al., 2013). Figure created with BioRender.com.

2.2.4 Modification techniques

Genetic engineering and chemical modification techniques can be used together to expand variety of potential applications using M13 in biomedicine (Chung et al., 2014). The self-assembly nature of M13 and their LC behaviour is a notable difference to other viruses and can be modified which expands the application potential even more (Devaraj et al., 2018).

2.2.4.1 Genetic engineering methods

Capsid protein genes of phages are modified via genetic engineering to display desired molecules, usually proteins, on the phage surface. It is a powerful tool to modify each coat protein copy, but excess mutations can hinder the packaging, replication, and assembly efficiency of the phage (Chung et al., 2014). Many different approaches have been developed for phage capsid engineering, display, and screening. Carmody *et al.* (Carmody et al., 2021) categorized the most remarkable ones as follows.

Phage display

Phage display was developed in the 1980s and is probably one of the most known and a common phage-related method ever developed (Scott & Smith, 1990; Smith, 1985). The method has been lucrative and led to discovery of countless antibodies for biomedical applications, like diagnostics and therapeutics (Alfaleh et al., 2020).

First in phage display, an amino acid (AA), peptide (Smith, 1985) or protein, such as antibody (Scott & Smith, 1990), sequence is fused to the phage capsid gene, and then this foreign gene product is displayed on the phage surface. Then phages with these different epitopes are used as a phage display library in affinity screening. Biopanning process (many rounds of affinity selection) is used to recognize those recombinant capsid sequences that strongly bind the desired immobilized target molecule, like antigen, using the phage display library (Alfaleh et al., 2020). Basic principles of affinity screening with phage display library are shown in Figure 6 (Alfaleh et al., 2020).

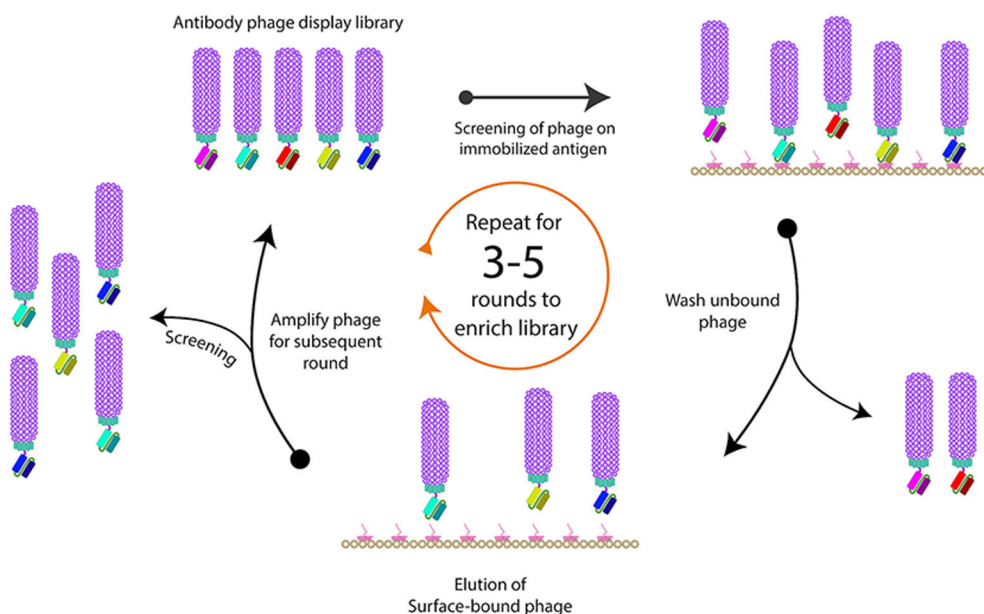


Figure 6. Basic principles of affinity screening with an antibody phage display library by Alfaleh *et al.* Sequences of different antibodies are fused to phage coat proteins and then displayed on the phage surface. Phages are used in a screen on immobilized target antigen. Then unbound phages are washed and surface-bound phages are eluted. This biopanning can be repeated 3–5 times to enrich the library and choose antibodies with the best affinity towards the antigen. Then these antigen-bound antibodies are identified (Alfaleh et al., 2020).

Homologous Recombination

Homologous Recombination (HR) is a natural phenomenon and well-established method for genetic engineering of phages in their bacterial hosts (Smith, 1988). In general, a recombinant dsDNA plasmid is built by cutting the plasmid DNA with restriction enzymes and then ligating synthetically designed sequence (gene) with ligands to plasmid. The synthetic sequence must be lined with homologous regions

in the phage genome. Then the recombinant plasmid is introduced into a host cell using transformation and the HR occurs. The gene is recombined into the phage genome during infection and progeny phages are produced (Møller-Olsen et al., 2022). With M13 having an ssDNA genome, the particle DNA is circular. Complementary strand synthesis forms a dsDNA circle during injection of the genome to the host cell (Smith, 1988).

In vitro assembly

Phage genome components are synthesized outside of the bacterial cell in the *in vitro* assembly. Components must have overlapping ends that can be ligated together to construct a recombinant phage genome (Carmody et al., 2021). Assembly of phages *in vitro* has been reported as early as 1960s' and 1970s' (Benchimol et al., 1978; Edgar & Lielausis, 1968; Konings et al., 1975). More lately, *in vitro* assembly has been used for example together with genetic and enzymatic manipulation to create recombinant phages displaying a potent human PCa cell-penetrating peptide on minor coat protein pIII (DePorter & McNaughton, 2014).

CRISPR/Cas9

The clustered regularly interspaced short palindromic repeats (CRISPR)-CRISPR-associated protein 9 (Cas9) system (CRISPR/Cas9) is one of the most known modern gene editing methods (Fard et al., 2024). Basically, an enzyme-RNA complex is used to precisely cleave or add a targeted gene to a specific location. From 2012 onwards, method has gained vast attention and has been used in countless number of applications in life sciences and biomedicine (Parkes et al., 2021). For example, with phages, the technology has been used to prepare a recombinant phage library by cleaving wild type genes from a pool of phages (Kiro et al., 2014). Duong *et al.* improved genomic editing rate of phages with CRISPR/Cas9 method and achieved editing rate of >99% for recombinant phage genes (Duong et al., 2020). In the CRISPR/Cas9 method, dsDNA is cut with Cas9 guideRNA (gRNA) which triggers endogenous DNA repair systems. Proteins are recruited either for non-homologous end-joining (NHEJ) for gene deletions and homology-directed repair (HDR) for adding an insert (Parkes et al., 2021). Figure 7 presents a simplified summary of genetic engineering by using CRISPR/Cas9.

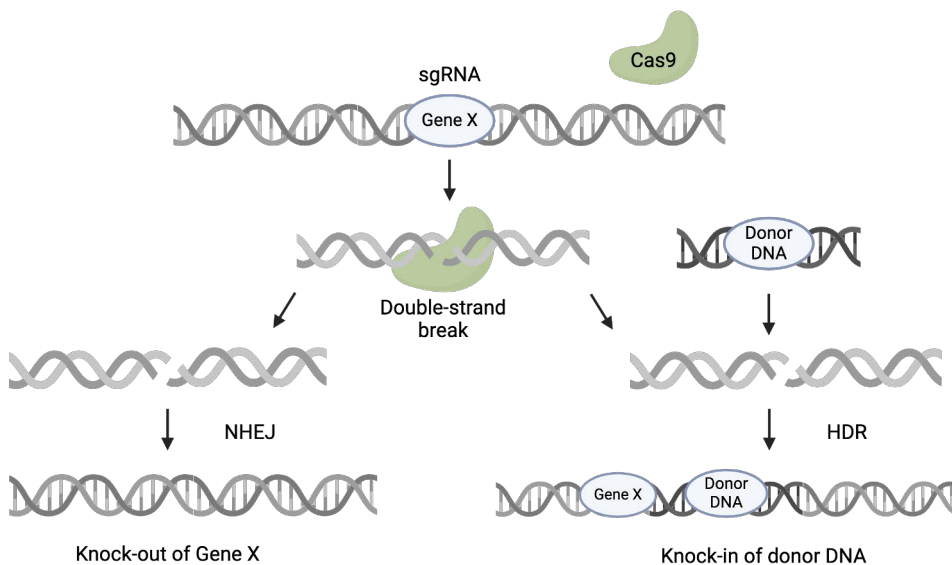


Figure 7. A simplified summary of genetic engineering by using CRISPR/Cas9. dsDNA is cut with Cas9 guideRNA (gRNA) which triggers endogenous DNA repair systems. Proteins are recruited either for non-homologous end-joining (NHEJ) for gene deletions and homology-directed repair (HDR) for adding an insert. Modified from Parkes *et al.* (Parkes *et al.*, 2021). Figure created with BioRender.com.

2.2.4.2 Chemical modification

Chemical modification can expand the use of phages in functional biomedical applications related to (bio)chemical sensors, bioimaging, and tissue engineering (Chung *et al.*, 2014). Synthetic functional groups are bound to specific sites of phages by chemical modification. The extent of modifications is limited by the availability and accessibility of reactive groups, their pKa, and conditions in the solution (Carmody *et al.*, 2021). However, when M13 is chemically functionalized the phage structure should retain while attaching the functional groups to the desired sites (Chung *et al.*, 2014). Often proteins attached to functional groups are rich of potentially reacting groups and their reactions may yield to undesired side products and modifications (Carmody *et al.*, 2021). Therefore, mild and facile chemosensitive reactions should be used in chemical modification of phages (Chung *et al.*, 2014). Though side reactions may occur even the modification conditions are designed to favour a certain reactive group (Abello *et al.*, 2007). Undesired modifications may reduce phage infectivity if they occur in important structural residues of the phage (Kim *et al.*, 2008).

The phage capsid consisting of proteins offers multiple options for bioconjugation via reactive functional groups. Amines at the N-terminus of proteins, lysine side chains, carboxylate groups at the C-terminus of proteins, aspartate and

glutamate side chains, thiol groups at cysteine side chains, phenol groups in tyrosine and histidine residues and aldehydes are all common targets for chemical modification. Thiols are the most reactive nucleophiles in proteins. Aldehydes are often used in cross-links to form chemically and thermally stable structures (Carmody et al., 2021). Cysteine and unnatural AAs have low-abundance and can be used in controlling the modification site (Marino & Gladyshev, 2010). Unnatural AAs also can be coded to phage genome to functionalize the desired sites of the capsid favourable to chemical modification (Sandman et al., 2000).

Various molecules can be attached to the phage surface with chemical modification. For example, luminescent dyes, chromophores, enzymes, and synthetic molecules can be used in different applications from biosensing to energy harvesting (Chung et al., 2014). Chung *et al.* reviewed methods for chemoselective modification and its applications in nanomedicine (Chung et al., 2014) and Shin *et al.* combined phage display and chemical surface modifications of M13 phage to build a virus-electrode interphase for detection of thrombin (Shin et al., 2023).

2.3 Biosensors

This thesis concerns phage-biosensors, which bioreceptor is a phage and transducers are optical. Therefore, the wide area of biosensors is delimited in this chapter to review optical and phage biosensors, and their applications in cancer detection.

2.3.1 General structure

Biosensors are analytical devices that are widely used for detection of different analytes, such as cancer biomarkers. They consist of three elements: 1) a component for biological recognition (bioreceptor), 2) a transducer, and 3) an electronic system that amplifies, processes the signal (Elois et al., 2023). The signal is then displayed in such a form that the result is understandable for the user. Schematic figure of biosensor structure and different types of bioreceptors and transducers are illustrated in Figure 8 (Naresh & Lee, 2021). Hereby, biosensors can be classified in various ways, and as always in classification, one biosensor may belong to many classes based on its construction.

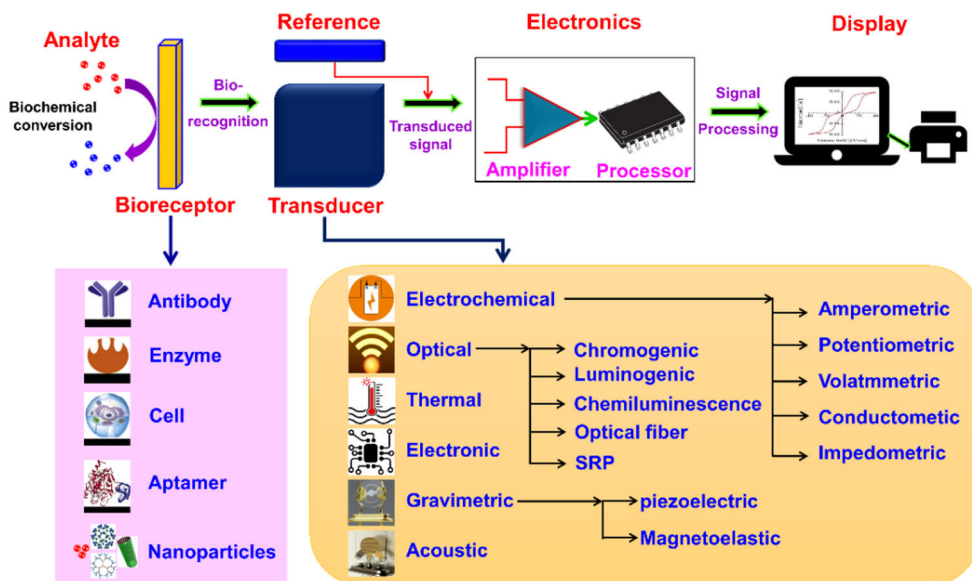


Figure 8. General biosensors structure and different options for bioreceptor and transducer by Naresh and Lee (Naresh & Lee, 2021).

2.3.2 Advantages and possibilities

Biosensor advances can overcome challenges related to conventional molecular detection methods, such as commonly used antibody-based or enzyme-based methods (Chadha et al., 2022). Current methods are expensive, have frequently low detection specificity, sensitivity and affinity, and they are sensitive for environmental conditions (Petrenko, 2018). New biosensor applications combine nanotechnology and clinical science and should overcome challenges related to conventional methods to compete with them. In the design phase of new biosensors, current challenges should be paid attention to, and attempts made to overcome them when pursuing the optimal end application to clinical use. Biosensors can be designed to detect biomarkers from previously challenging sample materials, such as urine and saliva samples, separate the biomarker from media, or detect multiple analytes at the same time (multiplexing). Clinical diagnostics could be simplified by biosensor-based rapid diagnostic tests (RDT) that are simple to perform with quick read-out. User-friendly operation, cost-effectiveness and large-scale production capabilities are the hallmarks in future diagnostic tests (Chadha et al., 2022).

2.3.3 Optical biosensors

Optical biosensors literally detect an optical change in signal measured from a biological medium. These are caused by interactions between sensor components

and target analyte. Optical biosensors have been used to detect various biomolecules, such as peptides, proteins and nucleic acids (Kim et al., 2016) and in different fields from biomedical detection to homeland security (Kamel & Khattab, 2020). They can be divided into multiple groups based on the transducer technology: chromogenic, luminogenic, chemiluminescent, optical fiber, and SPR, to mention a few (Naresh & Lee, 2021). Colorimetric and fluorescent biosensors can enable detection with a naked eye that makes them attractive options for different applications (Kamel & Khattab, 2020).

Another way for their classification is dividing them based on the use of labels in the sensor. Label-driven optical biosensors are often colorimetric or luminescent because either the bioreceptor or target molecules are labelled with colorimetric or luminescent tags. Their working principle is that the intensity change of the measured signal reveals the presence or absence of a target molecule. Advantage of label-driven optical biosensors is generally high sensitivity but are challenged by arduous labelling protocols and background signal from unspecific binding of label molecules. Label-free biosensors on the other hand, are comparatively simple and inexpensive because they do not use labelling of the bioreceptor or target molecules to convey the interactions from the detection reaction to measurable signal. They can be used in kinetic and quantitative measurements of molecular interactions for example via refractive index measurements. A major advantage of some label-free biosensors compared to label-driven biosensors is that they may not require large sample volumes. Their detection is based on signal changes by the molecular interactions corresponding to the surface density or concentration of the sample instead of direct analyte concentration, the recognition surface, or the recognition volume (Kamel & Khattab, 2020).

The optical signal is beneficial when compared to other physical signals because of their performance in biomedical applications. They have high sensitivity, robustness to various external factors, good stability, and low noise. They can be designed without complex sample pretreatment which could affect the target molecules (Chen & Wang, 2020). Optical biosensors are a very diverse group when compared to other biosensor transducer groups (Kamel & Khattab, 2020). The next chapter reviews commonly used transducer techniques with phage-biosensors.

2.3.4 Phage-biosensors

Properties of phages were reviewed in chapter 2.2 in more detail. Phage-biosensors have gained attention during last decades because they offer eco-friendly (Kim et al., 2023), durable and multifunction building blocks for developing new kind of nanomaterials and platforms for detecting various analytes (Brödel et al., 2018; Yang et al., 2013).

2.3.4.1 Optical phage-biosensors

Phages are known for their eminent capability to detect different bacterial pathogens due to their specificity towards their host. This prowess has been used in many applications to detect pathogens (Ahovan et al., 2020; Costa et al., 2023; Kulpakko et al., 2019; A. Singh et al., 2013). In addition, their advantageous properties have been and are utilized with increasing extents in various modern biosensors and analytical platforms. The most common optical transducers for phage-biosensors are luminescent and colorimetric (Ahovan et al., 2020).

2.3.4.1.1 Luminescent biosensors

Luminescent applications are widely accepted and used in biomedical detection. Phages can be combined with luminescence to improve desired factors such as sensitivity or durability.

Förster resonance energy transfer (FRET) is among widely used methods in biomedicine and bio-optical imaging. The phenomenon was reported for the first time in the 1940s. FRET has improved the spectral resolution and sensitivity of fluorescent detection applications (Kim et al., 2016). The basic principle of FRET is that non-radiative energy transfer appears by dipole-dipole coupling between an excited state donor (a fluorophore) and a ground state acceptor (a fluorophore or quencher). This happens with suitable spectral overlap and extreme proximity for the specific donor-acceptor pair. FRET can be used with nanoscale proximity detection, typically $\sim 1\text{--}10$ nm, and needs only simple benchtop equipment for the measurement (Algar et al., 2019). M13 phages have been used in FRET applications. Fernandes *et al.* increased selectivity towards target phospholipids by labelling M13 and using it as a donor in FRET study (Fernandes et al., 2004). Socher and Imperiali used M13 in their FRET-CAPTURE method to detect dynamic protein interactions and gained 20–30 fold increase in the FRET-fluorescence compared to traditional FRET-based measurements with minor background fluorescence and without washing steps. The main finding was high signal selectivity with elimination of false positive results (Socher & Imperiali, 2013).

Surface plasmon resonance (SPR) appears when electrons in metal are excited by the incident light with specific angle and wavelength. The total internal reflection of light weakens in these interactions and a minimum, SPR dip, occurs in the reflection spectrum. The refractive index, the minimum and a rotation of the angle of the light are changed when polarized light is used and target analyte, is immobilized to the metal surface (Falkowski et al., 2021). SPR is an outstanding option for a biosensor platform because it provides information of fundamental molecular interactions between the target and the bioreceptor. Additionally, it is label-free, does not need sample purification or enrichment, and enables direct detection of the target by utilizing high specificity and affinity of antibodies.

However, as a consequence of disadvantages of antibodies, such as laborious and expensive production, phages have offered a good alternative for them as a bioreceptor in SPR. Kim *et al.* reported a highly sensitive and selective SPR phage-biosensor binding to streptavidin (Kim *et al.*, 2016). However, suitability of the method was not tested with biological samples. Karoonuthaisiri *et al.* used M13 in SPR assay to detect *Salmonella*. Their main findings were low cross-reactivity and proof of M13 utility as a bioreceptor in a rapid and label-free SPR in detection of pathogens (Karoonuthaisiri *et al.*, 2014). Despite the detection limit was not as low as with some other methods in whole-cell detection, their results suggest that phages can be used in novel SPR-methods for detection of different targets. Hou *et al.* reported a phage-based SPR biosensor to detect carcinoembryonic antigen from serum. The biosensor reached ultrasensitive results being approximately 2000 times lower than conventional SPR (Hou *et al.*, 2023). This novel approach still requires more studies and validation before established to biomedical detection.

Surface enhanced Raman scattering (SERS) has been used in numerous applications to detect single molecules, biomarkers and performing molecular analysis. Since the 1970 it has been applied within different fields from forensics to medicine since 1970s. SERS is a vigorous spectroscopic method where molecules are attached to the metallic surface and Raman signal from them is prominently amplified. This yields a highly sensitive detection (Kim *et al.*, 2016). Lee *et al.* reported SERS-biosensor system using genetically engineered M13 for signal enhancement (Lee *et al.*, 2014). Practical applications with combining M13 phages to SERS method in bacterial detection and inactivation of *S. aureus* and *E. coli* were reported respectively by Wang *et al.* (Wang *et al.*, 2021) and Bi *et al.* (Bi *et al.*, 2023). In more detail, Bi *et al.* utilized the self-assembly of M13 to construct a phage-based nanocarrier for SERS (Bi *et al.*, 2023). However, fundamental limitation of SERS in biomedical detection is low selectivity with complex biological samples causing background signal and/or suppression of the analyte signal. Therefore, pretreatment and separation techniques are often required (Cialla-May *et al.*, 2024).

2.3.4.1.2 Colorimetric biosensors

Colorimetric biosensors quantify the color changes during the detection. The nanostructures can vary by size and periodicity depending on the biosensor construct. When they are illuminated, the specific wavelengths are scattered differently based on the interactions in the sensor. (Kim *et al.*, 2020). The read-out of the biosensor can be performed with spectrophotometers or even with smartphones which enable simple, sensitive, achievable and affordable detection applications (Peltomaa *et al.*, 2016).

Unique and versatile properties of phages have been utilized in many colorimetric biosensors (Kim *et al.*, 2020; Kim *et al.*, 2023; Lee *et al.*, 2021; Moon

et al., 2017). Especially controlled self-assembly of M13 and their LC properties has been applied in modern colorimetric biosensors and nanomaterials (Kim et al., 2020; Sawada, 2017). Colorimetric phage-biosensors have demonstrated competence in highly sensitive detection of target analytes and have been suggested to be a one option for constructing multiplexed sensors (Kim et al., 2020). Moon *et al.* genetically engineered M13 and fabricated a structural colorimetric sensor based on self-assembly of the phage to classify different antibiotics. Lee *et al.* used surface chemistry and genetically engineered M13 to construct a portable colorimetric detection test. Colour change of the sensor was based on self-assembly of engineered phages and results were experimentally verified for detecting volatile organic compounds (Lee et al., 2021). All these colorimetric phage-biosensors are quite recent methods and lack a clinical validation for biomedical analysis.

2.3.4.2 Phage-biosensor applications in cancer detection

Various applications have been reported lately harnessing phages to optical detection of various cancers. Much is expected from them and their clinical usability. For example, early cancer detection from liquid biopsies, like blood, urine and saliva, is one direction of development. Requirements for such applications are 1) high sensitivity, 2) specificity to exclusively bind the target analyte instead of the other similar analytes in the same liquid biopsy, 3) dynamic response including analyte concentrations in liquid biopsy both healthy and cancerous individuals, and 4) precision in detection with cases close to cut-off value of the analyte (Falkowski et al., 2021).

Methods enabling cancer detection from serum could be convenient because blood is routinely collected and analyzed in clinical laboratories. Zhan *et al.* designed an immunosensing platform using dynamic light scattering. M13 was used as a building block for assembling nanoparticles in detection of tumor marker alpha-fetoprotein from undiluted serum. The sensitivity with the developed platform was 165-fold lower than with traditional phage-based ELISA (Zhan et al., 2022). Wang *et al.* developed phage-immunosensor based on electrochemical impedimetric spectroscopy (EIS). They targeted vascular endothelial growth factor (VEGF) 165 from serum samples that have potential to be a therapeutic target in many malignant tumors (Wang et al., 2022). Colon cancer biomarker c-Met protein was detected rapidly and selectively from serum with electrochemical phage-biosensor by Pourakpari *et al.* (Pourakbari et al., 2022).

On the other hand, methods for patient-friendly urine-based detection of cancer have been developed. Mohan *et al.* used dual-ligand phage with electrochemical sensing to detect prostate-specific membrane antigen (PSMA) from synthetic urine (Mohan et al., 2013) and a bit later for detection of PCa cells expressing PSMA (Mohan & Weiss, 2015). However, newer publications from their technology are not

found. Bhasin *et al.* detected BCa marker DJ-1 from urine with engineered phages by measuring changes in electrical impedance (Bhasin *et al.*, 2020).

Methods enabling detection from multiple sample matrices can be useful in research and diagnostics. Zeng *et al.* used filamentous phage for colorimetric detection and quantification of microRNA (miRNA) biomarkers from plasma, tumor cells, and tissues. Mutations of miRNA increase in cancer (Zeng *et al.*, 2022). In turn, Nguyen *et al.* developed a multifunctional optical biosensor based on engineered M13 phages to detect volatile organic compounds (VOCs) and classify lung cancer from breath samples (Nguyen *et al.*, 2023).

2.4 Cancer

Cancer is an environmental, systemic and microenvironmental disease. Annually, almost 19 million new cancer cases occur and 10 million deaths worldwide (2022) (World Health Organization, 2024b). Typically cancer is a disease of people older than 50 years old but incident rates of early-onset cancers are alarmingly increasing (Ugai *et al.*, 2022). All in all, the global cancer burden is rapidly growing as a consequence of aging and growing population, and exposure to risk factors such as tobacco, alcohol, obesity and air pollution. World Health Organization (WHO) estimates an increase of 77% from 2022 to 2050 in cancer cases (World Health Organization, 2024a).

Outcome of the cancer patient depends on time of diagnosis, quality of diagnostics, cancer type, and effectiveness of the treatment. Especially advanced cancer and aggressive variants affect dramatically the prognosis and life quality of the patient (Connal *et al.*, 2023). This chapter introduces cancer as a disease, urological cancers, and diagnostics at general level, and underlines challenges and future prospects related to cancer detection.

2.4.1 Hallmarks of cancer

Hallmarks of cancer were introduced by Hanahan and Weinberg in 2000. They were six essential biological alterations of cell physiology needed in human tumour development: 1) sustaining proliferative signalling, 2) evading growth suppressors, 3) enabling replicative immortality, 4) activating invasion and metastasis, 5) inducing or accessing vasculature, and 6) resisting cell death (Hanahan & Weinberg, 2000). Same authors published an update 2011 and suggested two new hallmarks, 7) deregulating cellular metabolism, and 8) avoiding immune destruction, together with two enabling factors, 1) genome instability and mutation, and 2) tumour-promoting inflammation (Hanahan & Weinberg, 2011). Nowadays, these updates have been accepted as a part of hallmarks of cancer. In 2022, Hanahan published ‘new

dimensions' to earlier hallmarks and proposed again two new emerging hallmarks, 9) unlocking phenotypic plasticity, and 10) senescent cells, and two new enabling factors, 3) non-mutational epigenetic reprogramming, and 4) polymorphic microbiomes. These hallmarks of cancer and newest proposals are presented in Figure 9 (Hanahan, 2022).

From the original six hallmarks, capability to metastasize is a major factor in advanced cancer. After cancer hallmarks have been activated, a combination of genetic and epigenetic changes in the cell morphology and phenotype causes evolving of a neoplastic cell to a metastatic cell. During metastasizing a malignant cell migrates from its primary origin and establishes a metastasis to surrounding tissues or distant secondary organs (Seyfried & Huysentruyt, 2013). Metastasizing requires a vast chain of events. Four hallmarks of metastasis have been defined: 1) motility and invasion, 2) modulating the secondary location or local microenvironments, 3) plasticity, and 4) colonizing secondary tissues (Welch & Hurst, 2019). Cancer-related deaths are caused by metastatic disease in 90% of the cases. Thereby, it is the leading death cause in cancer patients (Connal et al., 2023).

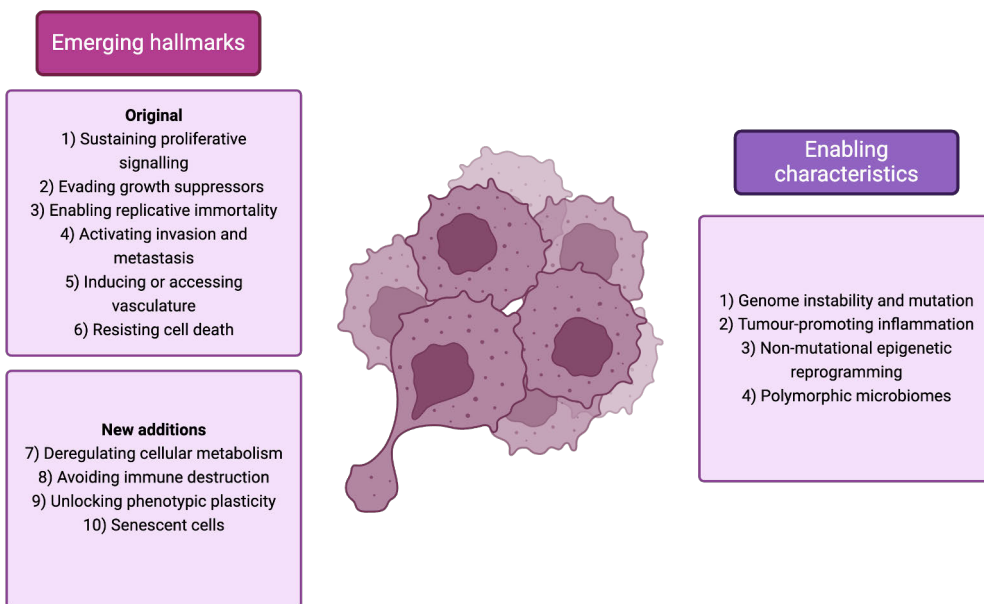


Figure 9. Original hallmarks of cancer and new additions. Modified from Hanahan (Hanahan, 2022). Figure created with BioRender.com.

2.4.2 Urological cancers

Urological cancers are cancers of the prostate, kidney, bladder, penis, and testis (Barber & Ali, 2022). Alias, these are tumours in the urinary system and male

genitals (Netto et al., 2022). The incident rates of urological cancers have increased globally for the same reasons as cancer incident rates in general. Especially cases of prostate, bladder and kidney cancer are increasing rapidly (Dy et al., 2017). Overview of urological cancers is presented in Table 1.

Epithelium of the urinary system extends from the renal collecting tubules to the urethral meatus. The cells of epithelium are highly specialized and known as the urothelium or transitional cells. Malignant transformation leading to cancer can happen in any part of the urothelium. More than 90% of cancers in the urinary system are transitional cell carcinomas (TCC) more often known as urothelial carcinomas (UC). Less common cancers are squamous cell carcinomas, small cell carcinomas, adenocarcinomas and benign neoplasms (Yaxley, 2016).

Table 1. Overview of urological cancers, their incidence and risk factors.

Cancer	Incidence globally (2022)	Incidence in men (2022)	Regional incidence	Risk factors
Bladder cancer (BCa)	9 th (World Health Organization, 2024c)	6 th (World Health Organization, 2024c)	Highest in Europe and Asia, lowest in Latin America and Oceania (World Health Organization, 2024c)	Smoking, male gender (Yaxley, 2016)
Kidney cancer (KCa)	14 th (World Health Organization, 2024c)	10 th (World Health Organization, 2024c)	Highest in North America, Western Europe and Australia (Du et al., 2020)	Alcohol consumption, overweight, and obesity (Du et al., 2020)
Penile cancer	30 th (World Health Organization, 2024c)	24 th (World Health Organization, 2024c)	Very low in high-income countries (0.1–1 per 100,000 men) (Thomas et al., 2021), but high incidence in South American, Asian and African countries (even up to 10% of male malignancies) (Coelho et al., 2018)	Human papillomavirus (HPV), infection, smoking, and poor hygiene (Thomas et al., 2021)
Prostate cancer (PCa)	4 th (World Health Organization, 2024c)	2 nd (World Health Organization, 2024c)	Lowest rates in Africa and Asia, highest rates in Northern America, Europe and Oceania (Wang et al., 2022)	Age, black race, obesity and diabetes (Wang et al., 2022)
Testicular cancer	27 th (World Health Organization, 2024c)	22 nd (World Health Organization, 2024c)	Rare, but highest incidence rates (3–10 per 100,000 men) in Western countries (Patrikidou et al., 2023), lower incidence rates but higher mortality in low-income countries, and in particular regions of Central and South America (Huang et al., 2022)	Low income, alcohol consumption, obesity and high cholesterol (Huang et al., 2022)

2.4.3 Clinical detection of cancer

Generally, cancer diagnostics follow a certain protocol from the clinical point of view. Symptoms, medical history and risk factors of the patient are reviewed. Physical examination, initial investigations (including laboratory tests and imaging), biopsy, and staging are performed if seen purposefully (Wilkinson, 2021).

Current detection methods can detect cancer after the tumour burden is large enough. Usually, the tumour is carcinogenic with a diameter of minimum 5 mm. Before that the premalignant lesions can be found via cancer screening or accidentally with imaging not related to cancer investigations (Wu et al., 2022). For molecular screening and diagnostics, laboratory tests, imaging and biopsies are the most interesting ones. Figure 10 demonstrates the current cancer development pipeline and diagnostic and treatment pathway in general.

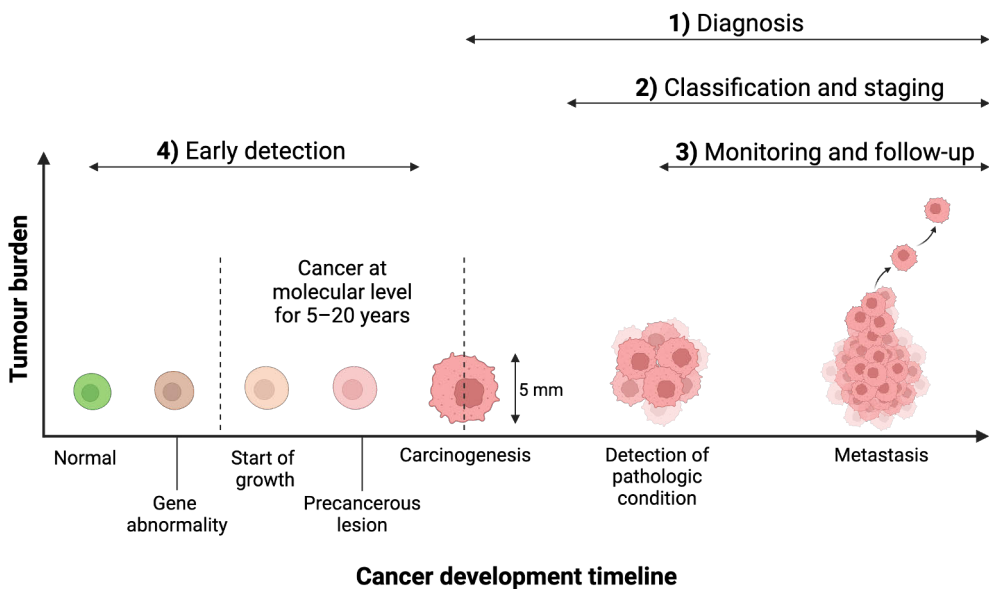


Figure 10. Cancer development pipeline together with diagnostic pathway. Modified from Wu *et al.* (Wu et al., 2022). Figure created with BioRender.com.

2.4.3.1 Imaging

Currently a wide selection of different clinical imaging methods for cancers is available. Imaging has been used routinely to locate and characterize tumours based on anatomic differences in size, shape, density, and water content (Farwell et al., 2014). Conventional methods have been used for years and they have different pros and cons. For example, endoscopy is an invasive method, and X-ray exposes a

patient to radiation. Positron emission tomography / computed tomography (PET/CT) and magnetic resonance imaging (MRI) can identify solid tumours but are not suitable for early-detection due to insufficient resolution and contrast to ratio (Li et al., 2022).

However, imaging methods are constantly developed and improved further to enable more sensitive cancer detection. For instance, 18F-fluorodeoxyglucose (FDG)-PET can characterize molecular changes in tumours and has enabled higher detection and staging sensitivity and specificity than anatomic imaging methods. PET is used not only for detecting cancer but follow-up of treatment response and characterizing tumour biology (Farwell et al., 2014). In addition, molecular and physiological information provided by MRI can improve cancer management (Li et al., 2022). Multiparametric MRI is a promising tool for PCa diagnostics and could reduce over diagnosing insignificant cancer (Stabile et al., 2020). However, high-tech imaging methods are expensive and not suitable for large-scale screening purposes.

2.4.3.2 Biopsy

A biopsy is a small sample collected from a tissue and observed under a microscope to identify the potential cancer cells (Sekhoacha et al., 2022). Biopsy is the “gold standard” in tumour profiling and needed in the majority of cancers to define the specific stage and type of cancer. It can be collected in multiple ways, such as through endoscopy or with a needle. Some challenges related to biopsies are too small sample volumes leading to misdiagnosis and inability to characterize the heterogeneity and clonal evolution of the tumour (Connal et al., 2023).

2.4.3.3 Molecular analysis

Molecular analysis of biomarkers is an important tool in effective cancer management. Detection and quantification of biomarkers can be used for early-stage screening, diagnostics, prognosis, and follow-up of cancer. However, characterization of these biomarkers is still a challenge because current methods lack required sensitivity and specificity (Kumar et al., 2023; Pal et al., 2022). Cancer-related biomarkers belong to various biomolecular groups present in human fluids, such as serum and urine (Pal et al., 2022).

Proteins can be abnormal or misexpressed in cancer cells or their presence can be a response to the cancer. However, the concentration of protein biomarkers is often extremely low, and their reliable detection can be hindered by other unspecific background proteins, they cannot be amplified for the detection, and they are highly sensitive for environmental factors (Kumar et al., 2023). Many cancer-related protein

biomarkers have been identified, such as commonly known PCa-associated prostate specific antigen (PSA) (Falkowski et al., 2021).

Nucleic acid biomarkers are a broad group of DNA and RNA markers for cancer detection (Kumar et al., 2023; Pal et al., 2022). Cell-free DNA (cfDNA) and circulating tumor DNA (ctDNA) may be released into the circulation by developing tumour cells and can be used as noninvasive biomarkers for cancer diagnostics and monitoring. Many technical challenges are remaining to detect them reliably, such as false-positive results due to low sensitivity and clinical applicability. mRNA is a clinically accepted biomarker for detecting and monitoring tumour cells. Irregular mRNA metabolism is related to cancer development and proliferation. In addition, short noncoding miRNAs are recognized as cancer biomarkers (Kumar et al., 2023). Moreover, cancer cells themselves and enzymes can be used to detect cancer (Kumar et al., 2023; Pal et al., 2022). Cancer cells can be classified directly from healthy cells based on abnormalities, such as proteins, enzymes, or specific enzymes, on their surface or within the cells. Endogenous or intracellular enzymic biomarkers for cancer have been identified. Enzyme activity in cells, tissues, and human fluids can be dysregulated or have abnormal functioning related to cancer. Human telomerase is the best-known enzymatic biomarker for cancer. It is upregulated in most of tumour cells (Kumar et al., 2023).

2.4.4 Prospects in cancer detection

Over the decades, development of detection methods has improved cancer screening and diagnostics remarkably. However, cancer remains as a major health problem and cause of death. This is due to low accuracy of current diagnostic methods which does not enable early detection of cancer (Bax et al., 2019; Pal et al., 2022). Below trends and prospects in modern cancer detection will be reviewed.

Early detection

The early detection of cancer improves treatment and prognosis of the patient (Bax et al., 2019; Pal et al., 2022; Weissleder, 2006). The 5-year survival rate is 90% for cancers diagnosed at stage 1, and if lesions are detected before malignancy, cancer can often be cured. Therefore, there is a massive opportunity to improve cancer management by identifying early-stage cancer biomarkers and developing new detection technologies for early detection of cancer (Weissleder, 2006). Understanding of biological structures and processes has provided information to support developing these methods (Bax et al., 2019). However, more research is still needed because there are plenty of unmet requirements for early detection. These new methods should be implementable to routine use, quick, pleasant for the

patients, affordable, and particularly sensitive and specific to be used in prognosis and early detection (Pal et al., 2022).

Liquid biopsies

Liquid biopsies are human bodily fluids, such as serum and urine, containing biomarkers (Connal et al., 2023; Flitcroft et al., 2022; Li et al., 2022). They are attractive options to detect and find new cancer-related biomarkers especially for early detection. However, there is a lack of established and standardized methods to study and analyse liquid biopsies (Li et al., 2022). Most of the proposed methods still need improvements, for example to their sensitivity, before they can be approved for clinical use (Connal et al., 2023).

Multiplexing and multi-cancer testing

Cancers are heterogenous by nature, and it is very unlikely that just a single biomarker could provide needed accuracy in cancer detection (Pal et al., 2022) or its staging. Therefore, detection of multiple biomarkers at the same time, *i.e.*, multiplexing, and combining omics data, has a great potential in developing new detection methods for cancer. Especially, aiming for early detection of cancer, multi-biomarker and omics approaches will be important. Another approach is to multiplex detection methods, such as hybrid imaging methods, where the staging is improved by combining results from imaging and molecular tests (Pal et al., 2022). In addition, cancer screening and diagnostics would benefit from multi-cancer tests that detect multiple cancers from a single test. Such tests could revolutionize cancer screening by providing rapid and early detection in cases where early cancer symptoms are yet rather unspecific. Particularly, they could improve detection of less prevalent cancers that are seldomly screened (Connal et al., 2023).

New biomarkers for typing and determining the stage of cancer

New detection methods and use of liquid biopsies enable identification of new cancer related biomarkers and more sensitive detection of known biomarkers in bodily fluids and tissues (Falkowski et al., 2021). Examples of new or potential cancer biomarkers are circulating tumor cells, cfDNA, DNA methylation, extracellular vesicles, cfRNA, platelets, and autoantibodies. In addition to cancer detection, these biomarkers can be used in risk stratification of patients, staging of cancer, early detection and better prognosis (Pal et al., 2022). However, more new biomarkers should be discovered together with development of new detection methods, to

overcome the challenges related to understanding cancer development, early detection and cancer management (Falkowski et al., 2021; Pal et al., 2022).

New technologies

Clinical detection of cancer poses many challenges related to limitations with current technologies, such as low sensitivity, complexity and large sample volumes, and external factors, such as need of technical expertise and high cost (Kaur et al., 2022). To overcome these challenges and improve cancer detection, new technologies must be developed. They should be highly sensitive and specific, rapid, user-friendly, stable, affordable, ecological, and minimally invasive (Kaur et al., 2022; Pal et al., 2022). Especially, nanotechnology and modern biosensor technologies are aimed to meet these requirements and improve early-stage detection and cancer management in the future (Kumar et al., 2023; Pal et al., 2022).

Patient-oriented and personalized approach

Due to the heterogeneity of cancers, cancer is a unique disease for each patient. The expression of genotypic biomarkers may vary, and different regions of the same tumour can have different characteristics. Therefore, a single biomarker cannot be used to describe cancer or its stage in an individual, and use of multiple biomarkers is most likely beneficial. However, this uniqueness can be used for personalised diagnosis, treatment and prognosis (Pal et al., 2022). For example, molecular imaging can integrate each patient's molecular and physiological information with anatomical information received from conventional imaging methods (Weissleder, 2006). Moreover, cancer diagnostics and treatment could be digitalized and personalized by fully integrating AI, imaging, molecular biomarkers and intermolecular networks in the future (Pal et al., 2022). Another approach to patient-oriented and/or personalized cancer detection is simple and affordable Point-of-Care (PoC) tests that can be operated outside the laboratory settings by the patient or healthcare practitioner. They could improve access to cancer screening also in low-income countries (Ng et al., 2022).

3 Aims

New molecular methods are needed to detect and classify cancer from non-invasive samples accurately, affordably and scalably. The thesis had three aims: 1) development of a phage-biosensor system; 2) explanation of the phenomena and biophysical properties during the detection with phage-biosensors; 3) assessment of applicability to detect single biomarkers and screen cancer from non-invasive urine samples with phage-biosensors.

The original publications had the following specific aims:

- I** To develop phage-biosensor for screening lethal PCa from urine samples and demonstrate the system with a model biomarker.
- II** To explain the phenomena of the phage-biosensor detection by studying the biophysical properties of the system with a model biomarker.
- III** To improve the selection process of phage-biosensor and assess capabilities of the system in classification of mCa from urine.

4 Materials and Methods

Summary of materials and methods is presented herein. More detailed information is given in the original publications (I–III).

4.1 Phages and microbes

Commercial Ph.D. -12 phage display library ($\sim 10^9$ unique sequences) containing 12-mer peptides fused to a minor coat protein (pIII) of phages was used as a base library for all biosensors. Selected phages were amplified in *E. coli* strain K-12 ER2738 (I–III). The library and *E. coli* were purchased from New England Biolabs (Ipswich, MA, USA).

4.2 Other biosensor components

Trimethylmethane dye, brilliant green (Figure 11), was purchased from Acros Organics (Geel, Belgium) and used as a complementary target for the phage in biosensors (I–III).

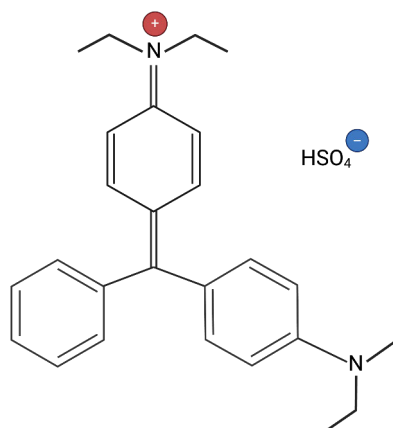


Figure 11. Chemical structure of trimethylmethane dye, brilliant green, used in the biosensor. Figure created with BioRender.com.

Europium label stock (3.9 mM europium chloride hexahydrate in combination with 2.3 mM 1-(2-Naphthoyl)-3,3,3-trifluoroacetone (NTA) and 2.3 mM Trioctylphosphine oxide (TOPO)) was used as a reporter solution for TRF in all publications (**I–III**). The dilutions of label components in assays varies and are reported in original publications in more detail. Label components were purchased from Sigma-Aldric (St. Louis, MO, USA).

4.3 Model biomarkers

C-reactive protein (CRP) was purchased from Sigma-Aldrich (St. Louis, MO, USA) and used in publication **I**. Green Fluorescent Protein (GFP) was purchased from Merck Millipore (Burlington, MA, USA) and used in publication **II**.

4.4 Clinical samples

Urine samples from patients with PCa, analysed in **I**, were obtained from the Helsinki Biobank as a part of PASSIONATE study (HUS/3372/2019) and from the Helsinki University Hospital as a part of DEDUCER trial (HUS/850/2017). Ethical approval for the use of samples and data related to them was obtained from the Institutional Ethics Committee of the Hospital District of Helsinki and Uusimaa. PASSIONATE is a retrospective registry-based study and DEDUCER is a prospective clinical trial related to urological malignancies. PCa was diagnosed with MRI as a triage test with complementary targeted \pm systematic prostate biopsies. Altogether, 96 urine samples were analysed of which 90 were distinguished less aggressive with Gleason Group (GG) 0–3 and 6 were classified lethal with GG 4–5.

Urine samples from patients with mCa, analysed in **III**, were obtained from the Helsinki University Hospital as a part of DEDUCER trial (HUS/850/2017) and from the Turku University Hospital as a part of BIOURICA study (ETMK 29/1801/2022). Control samples were collected from healthy volunteers based on their consent to participate in the study. Ethical approval for the use of samples and data related to them was obtained from the Institutional Ethics Committee of the Hospital District of Helsinki and Uusimaa and from the Ethical Committee of the Hospital District of Southwest Finland. BIOURICA is a prospective research study targeting novel urinary biomarkers for mCa with phage-biosensors. Altogether 74 urine samples were analysed of which 28 were mCa, 25 were cancerous without metastasis and 21 were non-cancerous controls. Cancerous samples were from patients with urological malignancies, mainly with PCa and KCa but patients with pancreas, bladder, penis, testis and retroperitoneal cancer were also included. Males represented 93% of the participants, due to included cancer types such as PCa, and females respectively 7%.

Cancers were diagnosed and classified with a biopsy and pathological analysis. In metastatic cases, imaging (CT, MRI or PET) was used to confirm the metastases.

All samples were collected, and experiments performed in accordance with relevant guidelines and regulations. The Ethical Standards of Declaration of Helsinki were followed in both studies using clinical samples (I, III).

4.5 Optical measurement methods

TRF was used in all publications (I–III) with settings of excitation wavelength of 340 nm and emission wavelength of 615 nm specific for europium and with a 400 μ s measurement window after 400 μ s delay time. Absorbance was measured with wavelength of 623 nm specific for the brilliant green dye (I–III), and with wavelength 610 nm specific for the resazurin sodium salt in the chemical assay (III). Absorbance spectrum was measured from 600 nm to 650 nm and luminescence was measured with excitation wavelength of 393 nm and emission wavelength of 509 nm specific for GFP (II). Spark multimode microplate reader from Tecan (Switzerland) was used for all TRF and absorbance measurements. LLG-uniREFRACTO 5 pro from LLG Labware (Meckenheim, Germany) was used for measuring refractive indexes (II).

4.6 Biopanning procedures

Biopanning is a process where phage clones are selected based on their affinity towards the target via affinity selection. In this study, we have developed a procedure to select bifunctional phages to be used in phage-biosensor. Herein, bifunctional phages are a pool of phages having affinity towards brilliant green dye, reporting in the detection, and towards target, either model analyte or cancer biomarkers in urine. The overall schematic for our biopanning process is presented in Figure 12.

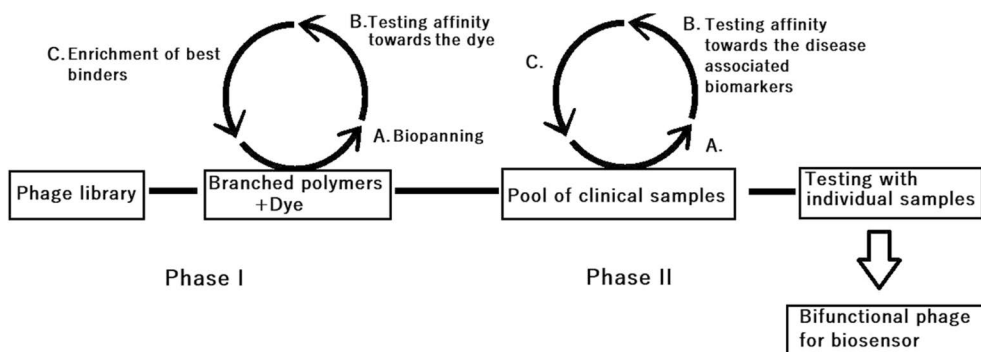


Figure 12. Schematic diagram of biopanning process to develop bifunctional phages to be used in biosensors. Figure was reprinted from publication I.

4.6.1 Coating with the target

Before biopanning, the dye solution, target analyte or samples are immobilized to a solid surface. Surfaces used in this thesis were hydrophilic polystyrene (Immuno Clear Standard Modules, Thermo Scientific) and chips consisting of highly branched polymers, lignin, and cellulose. The dye solution, diluted target analytes (**I**, **II**) or sample (**I**, **III**) were immobilized to the surface, rinsed to minimize unspecific binding and blocked with 2% BSA solution when necessary (coating). To gain sufficient specificity for the biosensor, samples were pools of cancerous samples used in coating. In publication **I**, pool of the most aggressive cases (GG 4–5) were used. After the first publication, we discovered that fractionizing the pools might yield greater specificity for our biosensors compared to using non-fractionized pools. In publication **III**, a sample pool of mCa was size exclusion-fractionized (illustra™ NAP-10 column with Sephadex™ G-25 DNA grade, GE HealthCare, Chicago, IL, USA) and used for coating.

4.6.2 Affinity selection of phages

In the first stage of biopanning, the ones having affinity towards the dye were selected from the base library of phages. A phage pool was incubated with the coated dye for 30 min with gentle shaking at room temperature (RT). Then unbound phages were washed serially and bound phages were amplified in *E. coli*. These amplified phages were used to repeat the selection with the dye. After 3 to 5 rounds of the first stage of biopanning, the phages were tested to have an adequate affinity towards the dye. The ability to form phage-dye complexes was compared between the selected phages and the base library by performing biosensor assays without the target and measuring results with both TRF and absorbance. These selected phages with adequate affinity towards the dye were used as a primed library to perform the second stage of biopanning in all experiments (**I-III**).

During the second stage of biopanning, the affinity selection towards the target from the primed library of phages was performed. The primed library was incubated with either the model biomarker or cancer pool, with gentle shaking in RT. After incubation, unbound phages were washed, and bound phages were amplified in *E. coli*. The second stage of biopanning was repeated from 2 to 4 times to gain adequate affinity towards target molecules. Detailed biopanning conditions, such as phage titers, incubation times, wash amounts and cycle amounts, are described in original publications (**I-III**). The detection performance of selected bifunctional phages was confirmed by comparing the assay results to the results with the base and the primed libraries.

4.7 Biosensor assays

In principle, biosensor assays were performed by adding biosensor components, the bifunctional phage, the dye, and label solution, to the 96-microplate wells. Analyte or urine sample dilutions were added in three replicates on top of the phage and dye. The label solution was added the last and after that assays were incubated with gentle shaking at RT before measurements. Phage amount, dye concentration, incubation time and measurement methods in the assays varied between the publications due to different optimal conditions for the biosensor in question. The main differences in assays between biosensors are presented in Table 2.

In publication **I**, phage-biosensor was developed to detect model analyte and was tested with dilution series of CRP. Another phage-biosensor was developed to screen lethal PCa (GG 4–5) from clinical urine samples and tested with diluted urine samples from patients with PCa (GG 0–5; n = 96). Both TRF and absorbance were measured from assays with phage-biosensors.

In publication **II**, a phage-biosensor developed to detect model analyte GFP was tested in various assay set-ups to study the biophysical properties in the phage-biosensor system. Biosensor assay was tested with dilution series of GFP: 1) without phages, 2) with primed library only having affinity towards the dye (control phages), and 3) with bifunctional phages having affinity towards the dye and GFP. Both TRF and absorbance was measured. After ensuring the affinity with bifunctional phage, assay was performed with it and broader dilution series of GFP to study the detection range. Absorbance spectrum of the system was measured with three different GFP concentrations and refractive indexes with a dilution series of GFP to study whether the detection has effect to it and compared to assay with control phages or without phages. Finally, lyotropic and thermotropic properties of the system were studied with assays with different titers of bifunctional phage and with incubation in different temperatures.

In publication **III**, phage-biosensor was developed to distinguish metastatic urological cancers, mainly PCa and KCa, from clinical urine samples and tested with diluted urine samples (n = 74) from patients with metastatic (n = 28) and nonmetastatic (n = 25) cancer and without cancer (n = 21). Samples were also measured with primed library (control phages). Absorbance was measured from assays.

Table 2. Assay conditions for different biosensors used in the publications. Symbols with superscript: *for TRF, ** for absorbance, ***for refraction, no superscript for TRF and absorbance.

Publication	Target	Target type	Measurement method(s)	Phage amount (pfu/mL)	Dye concentration (mM)	Sample diluent	Assay time (min)
I	CRP	Model analyte	TRF, absorbance	4.0×10^9	6	Saline	10*, 120**
I	Lethal PCa	Disease	TRF, absorbance	4.0×10^9	6	Saline	10*, 120**
II	GFP	Model analyte	TRF, absorbance, absorbance spectrum, luminescence, refraction	$2-12 \times 10^9$	0.036; 0.052	$0.01 \times$ PBS, 0.2% glycerol	60, 120, 240***
III	mCa	Disease	Absorbance	4.0×10^9	1	Saline	2-180**

4.8 Functioning principle of the biosensor

The functioning principle of the biosensor is likely based on competition between assay components. When target molecules, such as cancer-related biomarkers, are not present, the bifunctional phages (or a narrow pool of phages) interact with or bind to the dye molecules (inactive color), leading to a decrease in absorbance. In this case, the label molecules remain freely in the assay solution because they are not quenched by the dye and can emit a measurable TRF signal.

When target molecules are present, the bifunctional phages interact with or bind to them, allowing the dye molecules to be released into the solution (active color). As a result, the absorbance of the assay does not decrease. The dye molecules quench the label molecules and hinder their emission, causing the measured TRF signal to be low. The phenomena are illustrated in Figure 13.

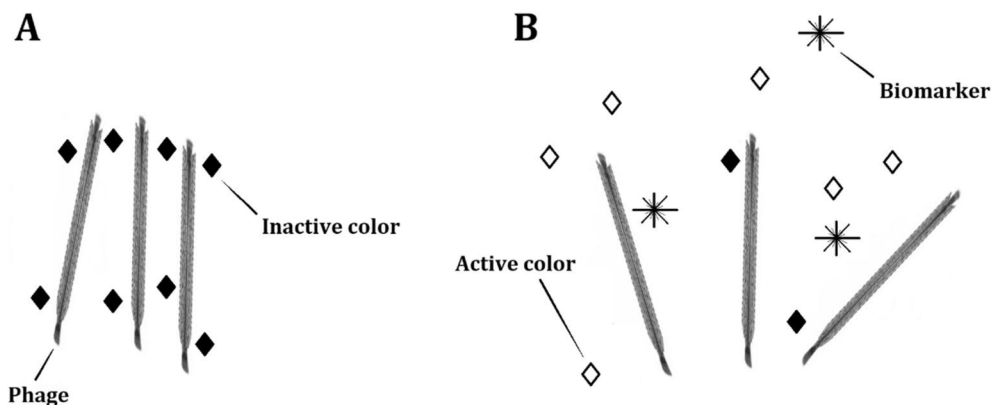


Figure 13. The functioning principle of biosensor. **A)** When target molecules are not present, the bifunctional phages interact or bind to the dye molecules (inactive color). This cause decrease in the absorbance. **B)** When target molecules are present, the bifunctional phages interact or bind with them, which leaves the dye molecules to the solution (active color). Figure was reprinted from I.

4.9 Chemical assay for cancer detection

Resazurin sodium salt was purchased from Sigma-Aldrich (St. Louis, MO, USA) and used in publications **I** and **III**. The chemical assay was performed by adding resazurin sodium salt (185 μM) and diluted urine samples to the 96-microplate wells. Samples were added in three replicates. Then, an europium label was added to each well. TRF signal was measured after 10 min (**I**) and 15 min (**III**), and the absorbance was measured after 5 min (**III**) of incubation.

4.10 Data analysis

All data analyses were performed with GraphPad Prism 9 for macOS (version 9.4.). The median of three replicate measurements for each sample (**I**, **III**) and mean of three replicate measurements for each dilution (**II**) was used in analyses. The linear combination of measurements was formed in publication **I**.

The mean TRF and absorbance values were normalized with the blank sample for each assay in publication **II**. The percentage of coefficient of variation (cv%) of three replicate measurements was calculated for Figures. To estimate the limit of detection (LoD), a standard curve was generated based on the measurement data and the concentration for the LoD (mean + 3 SD of the blank sample) was calculated from the equation of the curve.

In publication **III**, medians of samples measured with the biosensor were normalized with medians of the same samples measured with control biosensor. The method ROUT was used to identify outliers with the parameter “Q” set to “definitive outliers” (0.1). Unpaired t-test with Welch’s correction was used to calculate two-

tailed p-values and receiver operating characteristic (ROC) curve was plotted to estimate sensitivities and specificities with 95% CI for the biosensor and chemical sensor. In the significance evaluation of the results, p-values smaller than 0.05 were considered significant. Assay performances were estimated by comparing assay results to the clinical status of each study participant (**I, III**).

5 Results

5.1 Demonstration with model biomarker and screening lethal prostate cancer (I)

5.1.1 Detection of model biomarker CRP

The phage-biosensor was developed and tested with model analyte CRP before use with more complex clinical samples. Dye and CRP created a competitive microenvironment for the bifunctional phages, which have affinity for both molecules. The behaviour of phages influenced the europium label and its capability to emit signal. As shown in Figure 14, we found that the phage-biosensor quantitatively detected CRP as increasing CRP concentration caused decrease in measured TRF signal. The effect was steepest between CRP concentrations of 10–100 mg/L.

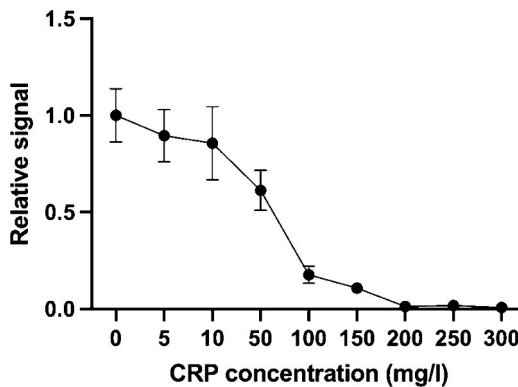


Figure 14. Quantitative phage-biosensor detection of CRP with TRF. Increase in CRP concentration caused decrease in measured TRF signal. Error bars are the coefficient of variance% of the signals from three replicate measurements. Figure was reprinted from I.

Respectively, the behaviour of phages had the opposite effect on the results measured by absorbance compared to those measured with TRF. The measured absorbance

values increased (in contrast to the decrease observed with TRF) as CRP concentration increased. The increase was steepest with CRP concentrations below 30 mg/L (Figure 15).

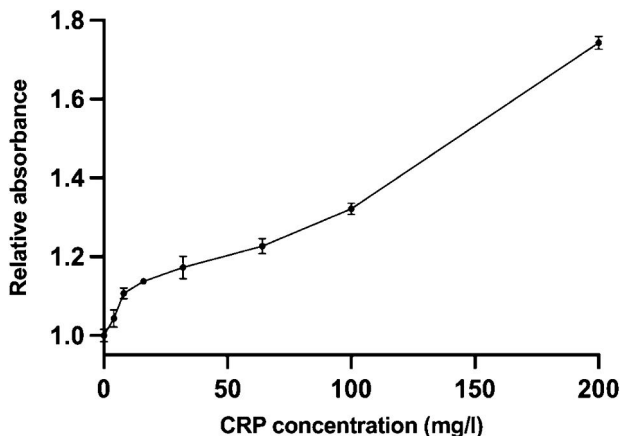


Figure 15. Quantitative phage-biosensor detection of CRP with absorbance. Increase in CRP concentration caused increase in measured absorbance. Error bars are the coefficient of variance% of the signals from three replicate measurements. Figure was reprinted from I.

5.1.2 Screen of lethal prostate cancer

Lethal PCa (GG4–5) was screened from clinical urine samples and distinguished from non-lethal ones (GG0–3) with phage-biosensor. The results were combined with chemical sensor results by using linear combination (Figure 16A). The system reached a calculated sensitivity of 80% and specificity of 75%. The result was statistically significant ($p = 0.014$) unlike the results based on PSA-values (Figure 16B) from the samples ($p = 0.2708$).

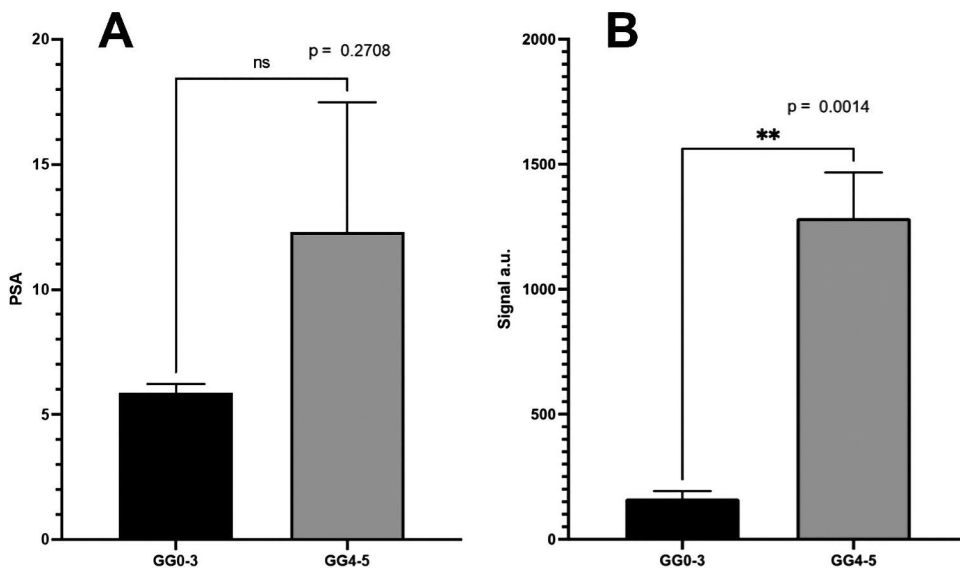


Figure 16. Comparison of PSA and phage-biosensor results in screening lethal prostate cancer (GG 4–5) from urine. Black bar shows PCa GG 0–3 ($n = 90$) and grey bar PCa GG 4–5 ($n = 6$). Error bars were standard error of mean (SEM). Clinical classification of samples was performed by MRI as a triage test with complementary targeted \pm systematic prostate biopsies. **A)** PSA-values measured with a conventional blood test. **B)** Linear combination of the measurements with phage-biosensor and chemical sensor (mean, $n = 96$, median of three replicates).

5.2 Biophysical properties of detection phenomena in phage-biosensor (II)

5.2.1 Quantitative detection of GFP with optical methods

Model analyte GFP was used to study biophysical properties of the phage-biosensor system. GFP was chosen because its specific optical properties (excitation 395 nm, emission 509 nm) are distinct from our biosensor system. Detection of GFP with phage-biosensor system was compared in three different assay set ups: 1) without phages, 2) with primed library having affinity towards the dye (after biopanning stage 1), and 3) with bifunctional phage having affinity towards the dye and GFP (after biopanning stage 1 and 2). Differences in assays are illustrated in Table 3. All set ups were measured with a GFP dilution series from 0 $\mu\text{g}/\text{mL}$ to 10 $\mu\text{g}/\text{mL}$, and at the same time with TRF and absorbance to ensure comparable results.

Table 3. Detection of GFP with a phage-biosensor system in three different set ups. Other assay components (the dye, label solution, and the GFP dilution series) remained the same except the phage.

Assay set up	No phage	Affinity towards the dye	Affinity towards both the dye and GFP	Legend colour and symbol in Figures 17 and 18
1	X			Grey ●
2		X		Blue ■
3		X	X	Green ▲
Explanation:	Assay without phages	Assay with primed library (monofunctional phage) having affinity towards the dye (after biopanning stage 1)	Assay with the bifunctional phage having affinity towards the dye and GFP (after biopanning stage 1 and 2)	

We found out that bifunctional phages clearly detected GFP quantitatively, and more sensitively than primed library or assay without phages (other assay components alone with the analyte). After ensuring GFP detection capability of bifunctional phage, we measured broader GFP dilution series from 0 $\mu\text{g/mL}$ to 100 $\mu\text{g/mL}$ with this biosensor to evaluate detection range for GFP and calculation of the LoD. The curves did not saturate either with TRF or absorbance, so the system was able to detect GFP within the measured concentration range. LoD with TRF was approximately 0.24 $\mu\text{g/mL}$ and with absorbance 10.2 $\mu\text{g/mL}$. These results are shown in Figure 17A with TRF measurements and with broader dilution series in Figure 17B. Respectively, the results with absorbance are shown in Figure 18A and with broader dilution series in Figure 18B.

In addition to differences in basic absorbance, we observed that bifunctional phages change the absorbance spectrum of the system. Results with three different GFP concentrations (0, 10, 100 $\mu\text{g/mL}$) are shown in Figure 19. The bifunctional phages also change the refractive indexes of the assay solution compared to the primed library, as illustrated in Figure 20.

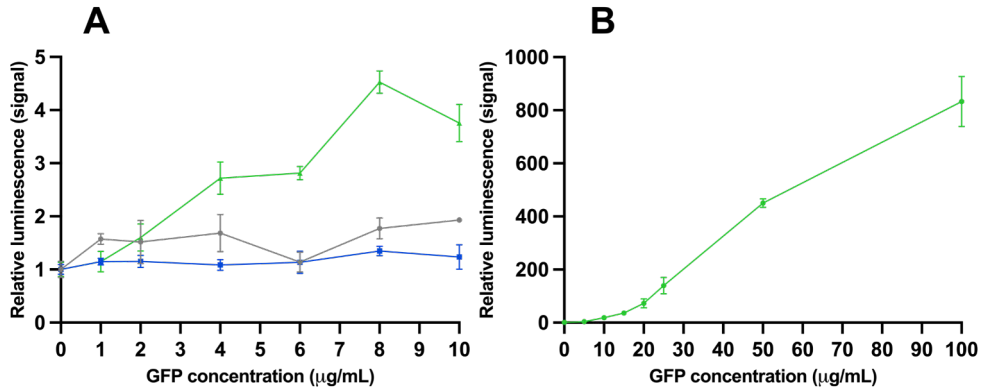


Figure 17. Quantitative TRF-based detection of GFP with phage-biosensor. **A)** Relative signal as a function of GFP concentration with three different assay set-ups: 1) without phages (grey line), 2) with primed library having affinity towards the dye (blue line), and 3) with bifunctional phage having affinity towards the dye and GFP (green line). Assay was measured after 120 min. **B)** Relative signal as a function of broader dilution series of GFP with bifunctional phage. Assay was measured after 60 min. The calculated LoD for GFP was 0.24 µg/mL. Error bars are the coefficient of variation (cv%) of three replicate measurements.

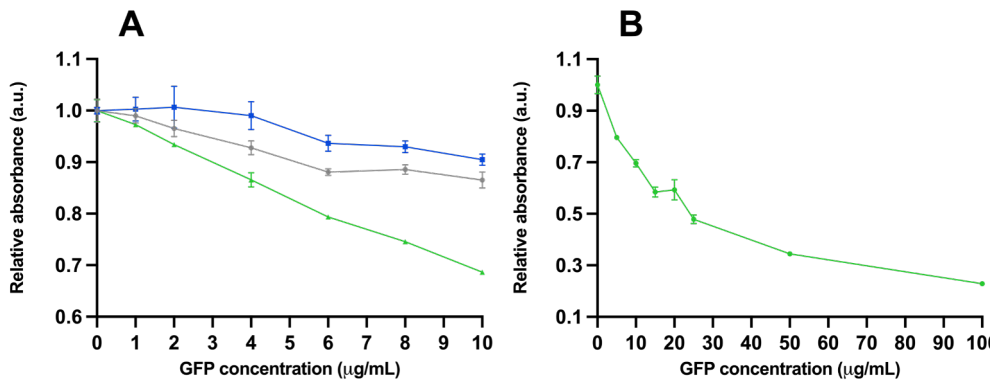


Figure 18. Quantitative absorbance-based detection of GFP with phage-biosensor. **A)** Relative absorbance as a function of GFP concentration with three different assay set-ups: 1) without phages (grey line), 2) with primed library having affinity towards the dye (blue line), and 3) with bifunctional phage having affinity towards the dye and GFP (green line). Assay was measured after 120 min. **B)** Relative absorbance as a function of broader dilution series of GFP with bifunctional phage. Assay was measured after 60 min. The calculated limit of detection for GFP was 10.2 µg/mL. Error bars are the coefficient of variation (cv%) of three replicate measurements.

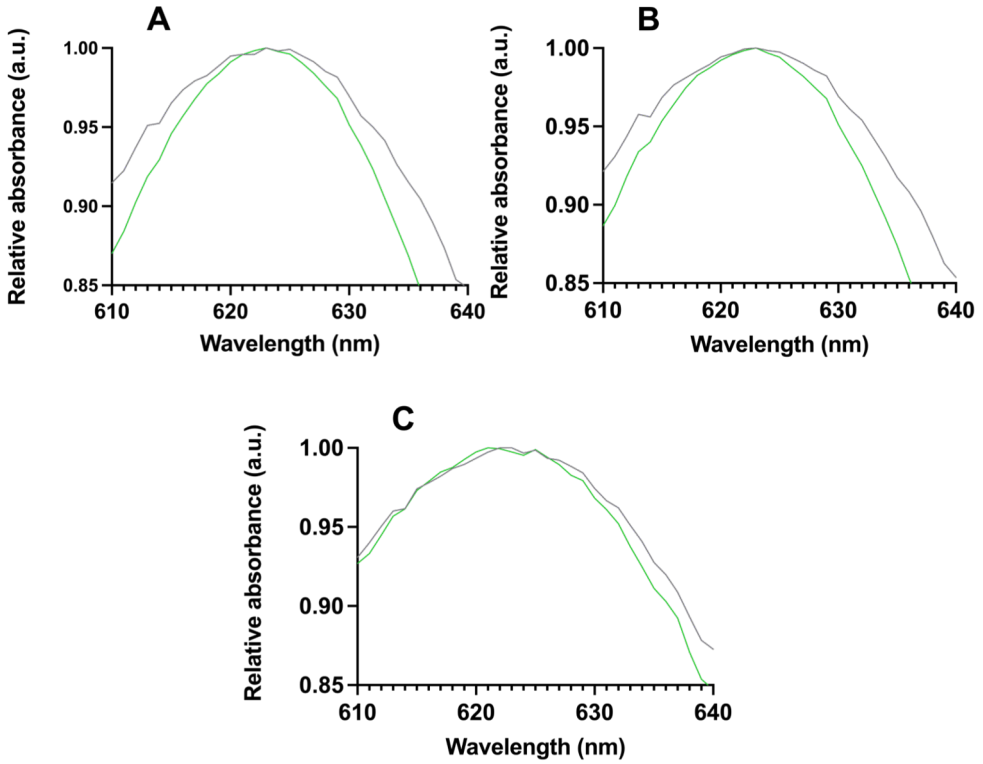


Figure 19. Absorbance spectrum measurement with phage-biosensor (green line) and without bifunctional phages (grey line) in three different GFP concentrations: **A)** 0 µg/mL, **B)** 10 µg/mL and **C)** 100 µg/mL.

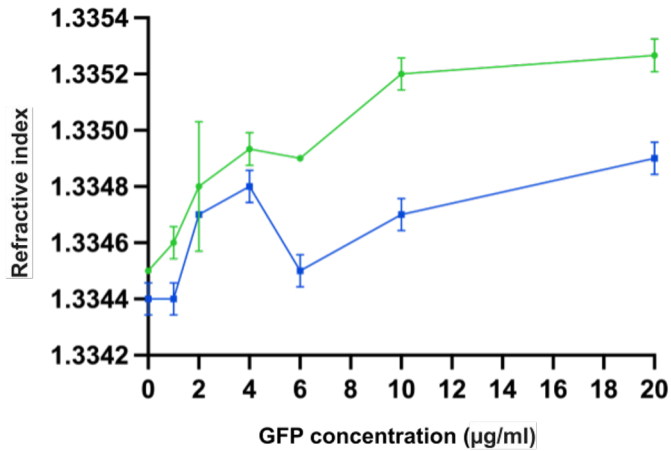


Figure 20. Refractive indexes measured from assay with phage-biosensor detecting GFP (green line, ●) and from assay with primed phage library (blue line, ■). Error bars are the cv% of three replicate measurements.

5.2.2 Lyotropic properties of phage-biosensor

Lyotropic behaviour, *i.e.*, concentration-dependent physical effects in liquids, of phage-biosensor was studied by measuring TRF and absorbance from assays without and with GFP and using different phage titers. Ratio between measurements with 0 $\mu\text{g/mL}$ and 25 $\mu\text{g/mL}$ GFP was calculated for each phage titer. Figure 21A shows that the optimal phage titer for GFP detection with TRF is 4.0×10^9 pfu/mL, and respectively Figure 21B shows that the optimal titer with absorbance is 1.0×10^9 pfu/mL. Thus, phage titer affects notably to the detection of GFP (with TRF ~ 40 -fold and with absorbance ~ 1.5 -fold), therefore we conclude that the phage-biosensor system likely exhibits lyotropic properties.

Additionally, phage titer influenced luminescence signal measured from GFP. The increase in average signal of GFP (25 $\mu\text{g/mL}$) above the background signal as a function of phage titer is shown in Figure 22.

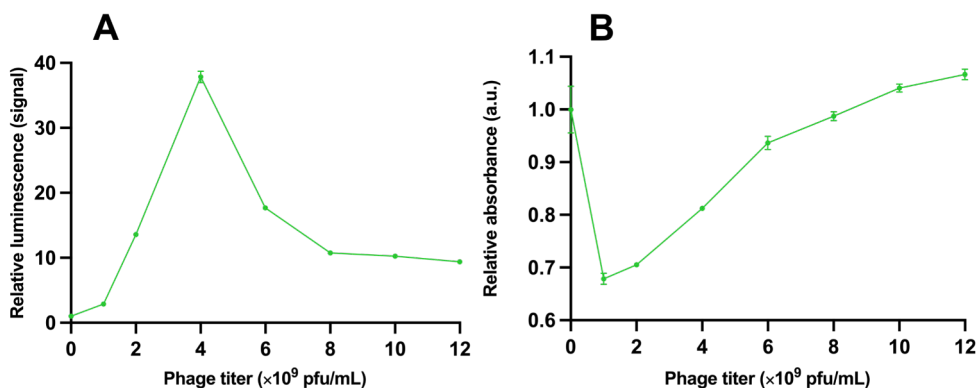


Figure 21. The relative ratio between GFP concentrations of 0 $\mu\text{g/mL}$ and 25 $\mu\text{g/mL}$ as a function of phage titer (pfu/mL). Figure **A**) shows results measured with TRF and **B**) with absorbance. Error bars are the cv% of three replicate measurements.

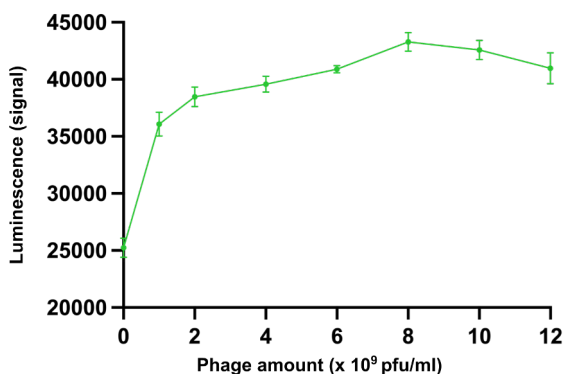


Figure 22. Luminescence signal of GFP (25 $\mu\text{g/mL}$) as a function of phage amount (pfu/ml). Error bars are the cv% of three replicate measurements.

5.2.3 Thermotropic properties of phage-biosensor

The effect of thermotropic properties of the phage-biosensor system was studied by performing biosensor assays with GFP in four different temperatures (+4 °C, RT, +37 °C and +50 °C). The incubation time and temperature have a clear effect on assay performance. With TRF measurements (Figure 23A), after 60 min incubation the ratio between concentrations 0 $\mu\text{g/mL}$ and 25 $\mu\text{g/mL}$ was ~ 12 -fold at +50 °C and only ~ 2 -fold at +4 °C. This effect started to appear after 15 min of incubation and increased up till 60 min. With absorbance (Figure 23B), after 30 min incubation the ratio between concentrations 0 $\mu\text{g/mL}$ and 25 $\mu\text{g/mL}$ was ~ 0.5 -fold at +50 °C and only ~ 0.65 -fold at +4 °C. On the contrary to results with TRF, with absorbance the effect started to disappear after 30 min.

In more detail, incubation time of 30 min and above yielded statistically significant results at +4 °C ($p < 0.0001$) and at +50 °C ($p = 0.023$) with TRF measurements (Figure 23A). Incubation time of 30 min and above yielded statistically significant results at +4 °C ($p < 0.0205$) and time of 10 min and above at +50 °C ($p = 0.015$) with absorbance measurements (Figure 23B). With the absorbance results at +50 °C the significance of results disappeared after 60 min of incubation when compared to other temperatures except +4 °C.

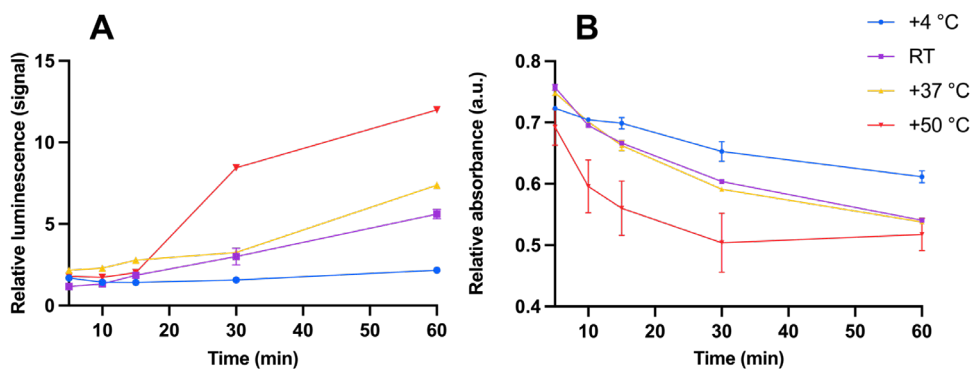


Figure 23. Effect of incubation time and temperature on the phage-biosensor system. Ratio between GFP concentrations 0 $\mu\text{g/mL}$ and 25 $\mu\text{g/mL}$ as a function of time in different temperatures (blue line: +4 °C; purple line: RT; yellow line: +37 °C; red line: +50 °C). **A)** presents the results measured with TRF and **B)** with absorbance. Error bars are the cv% of three replicate measurements.

5.3 Improved biopanning protocol and classification of metastatic cancer (III)

5.3.1 Major changes in methods

There were major changes in affinity-selection, phage-biosensor assays and data analysis of the results in this study when compared to corresponding reported in studies **I** and **II**.

Earlier in affinity selection, we attached diluted urine sample pools on the surface and performed biopanning directly against them. These samples contained all possible biomarkers present in the pool and a massive number of molecules and biomarkers not related to cancer or metastases. In this study, sample pools were size-exclusion fractionized with gel-purification columns which reduced the number of biomarker-masking molecules in biopanning (meaning less targets for the phage in affinity-selection) and enhanced possibility to select phages having affinity towards the specific metastasis-related biomarkers. Affinity-selection towards fractionized samples also yielded a larger number of phage candidates ($n = 29$) when compared to an earlier process that usually yielded less than 10 candidates which improves the chance to find working or the most effective biosensor. Additionally, separating of sample molecules into size-groups may help in biomarker identification later.

Another improvement was in phage-biosensor assays. Longer measurement time was used than earlier when the phage-candidates were evaluated, and biosensor assays performed. Assays were incubated 3 hours and measured in multiple time points, like every 5 min, to reveal an optimal time point for reading. An example from our earlier studies is that assays were measured every 5 min only during the first 15 min and then every 30 min.

In data analysis, we have earlier used either signals from raw data or standardized signals towards saline. In this study, we standardized signals from measurements with phage-biosensor to signals measured a primed phage library. This increased the classification power of the system.

5.3.2 Chemical sensor for cancer

The same chemical used in publication **I** as a part of screening lethal PCa with TRF was measured with a sample cohort in **III**. However, we measured absorbance instead of TRF. As shown in Figure 24A, based on absorbance cancerous samples ($n = 53$) were distinguished significantly from non-cancerous ($n = 21$) ($p < 0.0001$), with area under curve (AUC) of 0.73 (Figure 24B). Calculated sensitivity for the chemical sensors was 71% (95% CI 50–86%) and specificity was 75% (95% CI 62–85%).

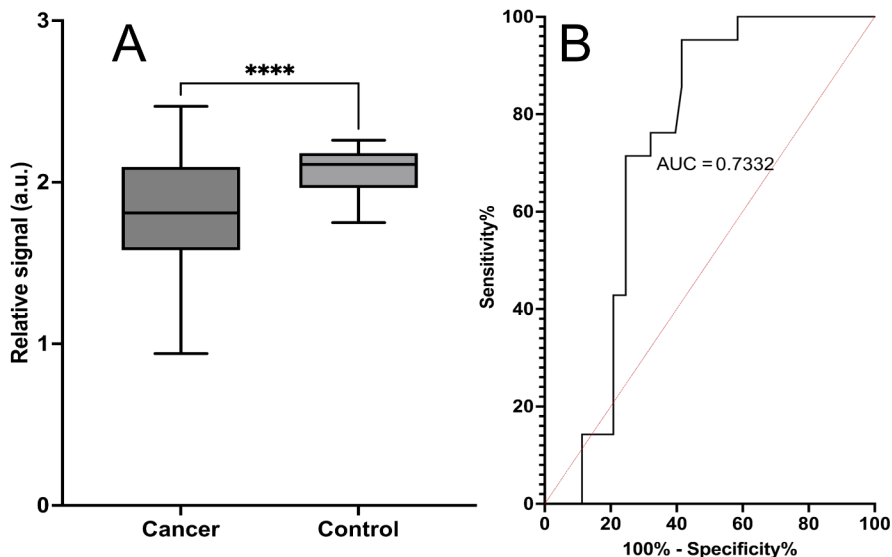


Figure 24. Chemical sensor for cancer detection from urine. **A)** shows signal mean of three replicate measurements, with SEM as error bars between cancerous ($n = 53$) and non-cancerous ($n = 21$) samples. Difference between these two sample groups was significant ($p < 0.0001$). **B)** shows the ROC curve with AUC of 0.73. The calculated sensitivity for the assay was 71% and specificity 75%.

5.3.3 Phage-biosensor for metastatic cancer

mCa ($n = 28$) was significantly distinguished ($p = 0.0002$) from non-metastatic cancerous and non-cancerous control samples ($n = 46$) with developed phage-biosensor (Figure 25A). The system reached a calculated sensitivity of 70% (95% CI 55–81%) and specificity of 79% (95% CI of 60–90%) with AUC = of 0.77 (Figure 25B). The same analysis was performed by excluding non-cancerous control samples from the analysis to ensure the classification between metastatic ($n = 28$) and non-metastatic cancer ($n = 25$) samples. The result was that the statistical significance remained in classification (Figure 26A), but it decreased ($p = 0.0017$). However, specificity abided the same (79% with 95% CI 60–90%) and decrease in other parameters was moderate: AUC decreased from 0.77 to 0.75 and sensitivity decreased from 70% to 68% (95% CI 48–83%) (Figure 26B).

Our studies of the phage-biosensor system have shown that the kinetic behaviour of the system is highly dependent on the biosensors and the target. In present study, we analysed the kinetic behaviour of the phage-biosensor with different samples. The colour formation in the phage-biosensor assay as a function of time was smaller for the metastatic sample than for the non-metastatic cancerous sample and the non-cancerous control sample. The slope of simple linear regression was for them respectively -1.2×10^{-4} , -7.1×10^{-4} , and -6.8×10^{-4} over the whole measurement

window of 180 min (Figure 27A). In particular, the change was more dramatic during the first 60 min of measurement because the slopes had opposite directions. Metastatic sample had positive slope of 5.6×10^{-4} whereas both non-metastatic cancerous and the non-cancerous control samples had negative slopes of -2.1×10^{-3} , and -1.4×10^{-3} (Figure 27B).

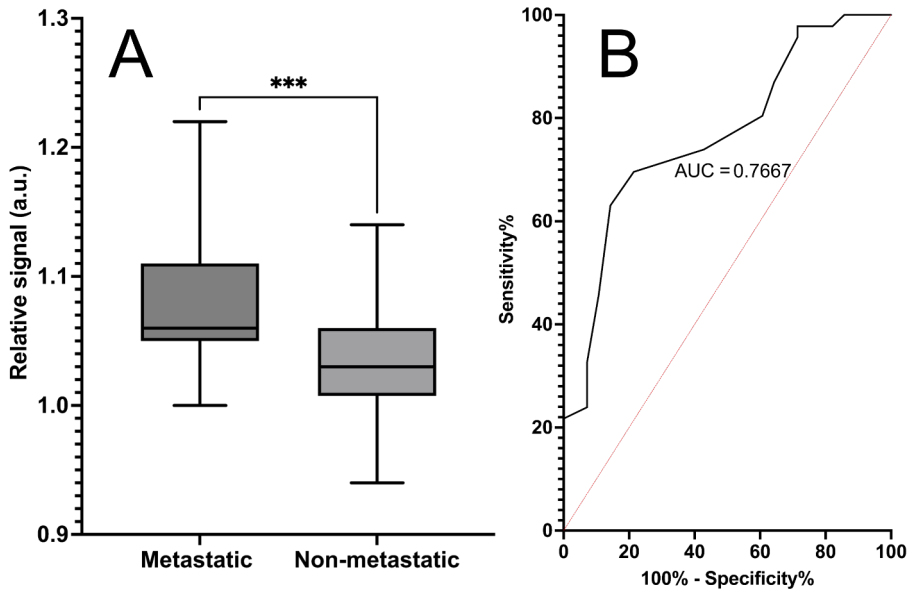


Figure 25. Phage-biosensor for metastatic cancer (mCa). Absorbance was measured from assays with bifunctional phage and primed library (control). **A)** Difference between metastatic ($n = 28$) and non-metastatic samples ($n = 46$) ($p = 0.0002$). Y-axis displays standardized means of signal of three replicate measurements, with SEM as error bars. Signals were standardized by dividing the signals measured with the bifunctional phage with the signals measured with the control phage. **B)** Displays the ROC curve with AUC of 0.77. Phage-biosensor reached sensitivity of 70% (95% CI 55–81%) and specificity of 79% (95% CI of 60–90).

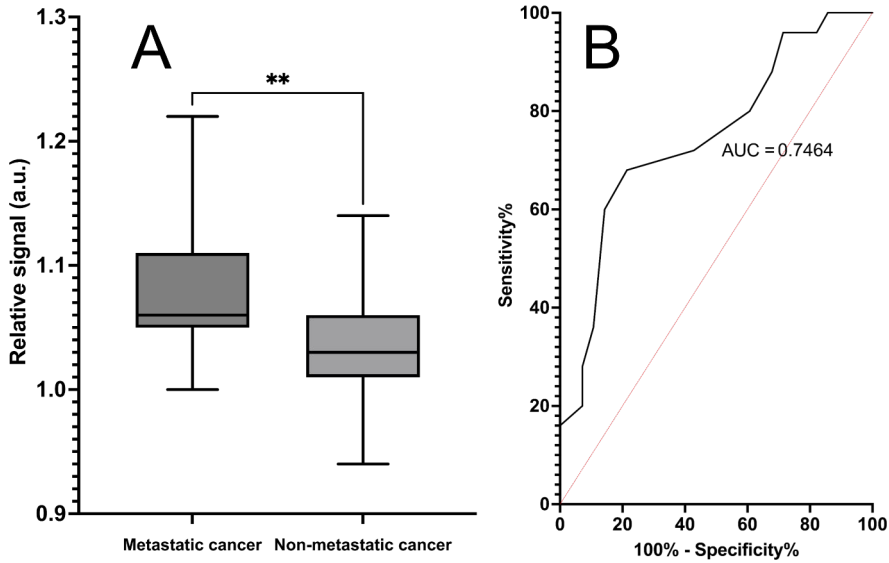


Figure 26. Results from phage-biosensor for metastatic cancer (mCa) when non-cancerous control samples were excluded from the analysis. Absorbance was measured from assays with bifunctional phage and primed library (control). **A)** Difference between metastatic (n = 28) and non-metastatic cancer samples (n = 25) (p = 0.0017). Y-axis displays standardized means of signal of three replicate measurements, with SEM as error bars. Signals were standardized by dividing the signals measured with the bifunctional phage with the signals measured with the control phage. **B)** Displays the ROC curve with AUC of 0.75. Phage-biosensor reached the sensitivity of 68% (95% CI 48–83%) and specificity of 79% (95% CI of 60–90%).

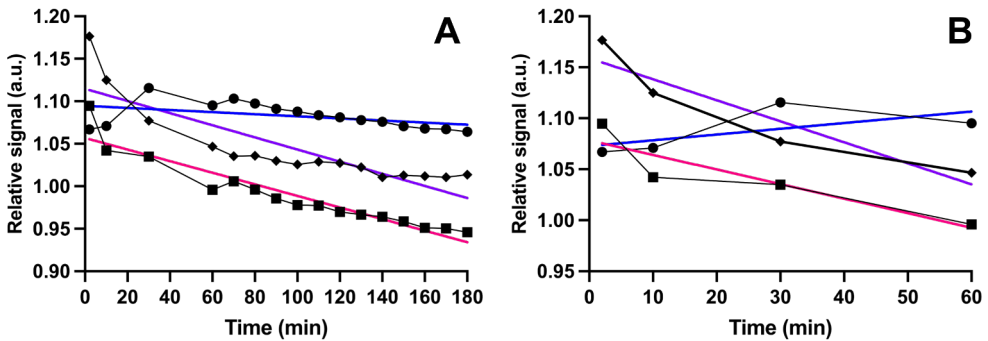


Figure 27. Colour change, *i.e.*, kinetic behaviour, of the phage-biosensor with a metastatic sample (●), non-metastatic cancer sample (◆) and non-cancerous control sample (■) as a function of time. The blue line displays the slope for relative colour change for the metastatic sample, the purple line for the non-metastatic and the pink line for the non-cancerous sample. **A)** A slope of linear regression during whole measurement time of 180 min was smaller for the metastatic sample (-1.2×10^{-4}) than for the non-metastatic (-7.1×10^{-4}) and non-cancerous (-6.8×10^{-4}) samples. **B)** A slope of linear regression during the first 60 min of measurement was positive for metastatic sample (5.6×10^{-4}) and negative for non-metastatic (-2.1×10^{-3}) and non-cancerous (-1.4×10^{-3}) samples.

6 Discussion

6.1 Clinical samples

Publications **I** and **III** used clinical urine samples in biosensor assays. In publication **I**, two cohorts were combined containing PCa samples with GG 0–5 and analysed together with non-cancerous control samples. All samples were collected between 2017–2020. In publication **III**, also two cohorts were combined containing metastatic and nonmetastatic cancer samples and analysed together with non-cancerous control samples. All samples were collected between 2017–2023.

All the original samples were processed and diluted at the same time. Use of different cohorts in biosensor testing proved that sampling time, sampling location, or storage time of urine (years) did not affect the results. Non-invasiveness of urine and its good shelf life are clear advantages for the method because new detection methods of cancer should be minimally invasive and stable (Kaur et al., 2022; Pal et al., 2022).

Limitations with the clinical samples were relatively small sample size (<100 samples in **I** and **III**) in cohorts, not age matched the control samples (**I**, **III**) and gender imbalance of the samples (93% male, 7% female in **III**). However, urological cancers are more prevalent in male (Barber & Ali, 2022; Siegel et al., 2018; Wang et al., 2022; Yaxley, 2016). Therefore, it can be stated that imbalance between genders does not distort the results remarkably. There was no correlation between the assay results and gender.

6.2 Biopanning

Biopanning is a process where phage clones are selected based on their affinity towards the target via affinity selection. Basically, it is a simple procedure applied in biomedical studies widely for decades, especially in the phage display method (Alfaleh et al., 2020; Scott & Smith, 1990). In general, different peptides, proteins or antibodies are displayed on the phage surface and the ones having affinity to target analytes are amplified for further use. The biopanning protocol used in this thesis follows the same principle, but the used original phage library is commercial and therefore, the displayed peptides are not designed specifically for this study.

However, the library contained a wide selection, $\sim 10^9$, of random peptides with high complexity providing sufficient basis for affinity selection of phages based on the achieved biosensor performances.

Before two-stage biopanning, target molecules were immobilized either to chip or polystyrene solid surfaces. The used chips were highly branched and constructed from lignin and cellulose. They were mainly used in stage I for coating the dye that did not bind to polystyrene. The used polystyrene wells were hydrophilic and targeting proteins and especially glycoproteins. This was intentional because model analytes targeted in this study were proteins (CRP, GFP), and many cancer biomarkers are proteins (Falkowski et al., 2021). In addition, the samples used for coating varied between the studies. In **I**, only a pool of urine samples with aggressive PCa was used for coating, and just one biopanning round was performed to yield the biosensor. In **III**, we aimed to improve the selection process of phage-biosensors, and therefore we size-fractionized the metastatic sample pool before coating both chips and polystyrene. Biopanning was performed against all the fractions and amplified biosensor candidates were tested to find the most specific one. Fractionizing most likely added the number of biomarkers presented for phages during affinity selection instead of binding biomarkers only from the full pool with excess of biomolecules and hindering unspecific molecules.

Many phage-display and phage-biosensor applications aim to have one highly specific phage clone towards the target analyte (Bhasin et al., 2020; DePorter & McNaughton, 2014; Mohan et al., 2013; Pourakbari et al., 2022; Wang et al., 2022; Zhan et al., 2022). Our biopanning protocol differs from these approaches and solely narrows down the number of phage clones during affinity selections. At the end, our biosensor contains a pool of phages with a few epitopes having affinity towards the dye molecule and target-specific biomarkers. Basic phage-display protocols repeat affinity-selection 3–5 times (Alfaleh et al., 2020). In this study, the first stage biopanning was already repeated 3–5, and then the second stage biopanning was repeated 2–4 times. Altogether, affinity selection was performed 5–9 times that is more than in basic phage display. However, we have noticed that repeating the second stage too many times impairs the performance of the phage-biosensor. This is most likely due to excessive narrowing of the phage pool from the original phage library and some necessary phage epitopes either towards the dye or target analyte were lost.

Overall, developed biopanning protocol is straightforward when compared to other modification techniques of phages (Carmody et al., 2021; Chung et al., 2014). It could offer a new technology to develop rather quickly phage-biosensors targeting various analytes, such as cancer biomarkers, and meet requirements of low-complexity, robustness, easy mass-production, and low costs (Kaur et al., 2022; Kumar et al., 2023; Pal et al., 2022).

6.3 Biosensor assays

6.3.1 Detection of model analytes

Aims in **I** and **II** included detection of model analytes with a phage-biosensor system. The quantitative detection of model analytes, CRP in **I** and GFP in **II**, was confirmed by measuring TRF and absorbance from dilution series of the single analyte with the developed phage-biosensor (**I**, **II**), with primed library, and without any phages (**III**). The main finding was that the two-stage biopanning process can be used to develop bifunctional phages which can further detect model analytes in the presence of the reporting dye molecule in the biosensor system. CRP, a clinical biomarker related to inflammation and infection, was detected at clinically relevant level (Sproston & Ashworth, 2018).

However, the cross-reactivity was not studied. Therefore, the analytical specificity towards the model analytes should be confirmed by repeating assays with other proteins. It is known that biomolecules, such as antibodies, have cross-reactivity in biomedical tests (Dias et al., 2016). Both TRF and absorbance had a quantitative response to analyte concentration, but TRF was around 10-fold more sensitive than absorbance. This is due to a sensitive nature of lanthanide label emitting TRF (Lakowicz, 2006). On the other hand, absorbance-based detection can enable interpretation of the result with a naked eye which is an attractive option for different biomedical applications. Even though, usually colorimetric and fluorescent methods are label-driven (Kamel & Khattab, 2020), in this case the assays can be considered as label free. Labelling of molecules are not needed, and the lanthanide label and the dye molecule are freely soluble in the homogenous assay solution. Therefore, our method combines the advantages of highly sensitive label-driven biosensors and less arduous label free biosensors (Kamel & Khattab, 2020).

Colorimetric detection of our phage-biosensor had kinetic behaviour and the color in the assay intensifies or diminishes in a few hours before the peak. This phenomenon was noticed already during **I**. However, one major observation in **II** was occurrence of the kinetic behaviour with TRF-based detection as well. This was applied to colorimetric and TRF measurements in **III**. Increase in the number of measurement-timepoints enabled more detailed analysis of behaviour of the biosensor and finding optimal measurement timepoints with both detection methods. Hence, biosensor performance, clinical sensitivity and specificity can be optimized by studying the assay conditions throughout.

6.3.2 Biosensor-based detection of PCa and metastases

Results from **I** and **III** proved the applicability of the phage-biosensor system to detect and distinguish cancers from clinical urine samples. In **I**, aggressive PCa was screened with sensitivity of 80% and specificity of 75%, and in **III**, mCa was distinguished respectively with sensitivity of 70% and specificity of 79%. The results were achieved via rather simple and quick fluorescent and colorimetric measurements which are attractive options for healthcare (Kamel & Khattab, 2020).

Reached sensitivity was higher for PCa biosensor than for metastatic biosensor. However, specificities were vice versa. The results were a combination of biosensor measurements and a chemical sensor measurement in **I**, but not combined in **III**. Possibly the sensitivity and specificity of the metastatic biosensor could be increased by analysing some measurements together. Combining different clinical data and results is a promising alternative for modern cancer detection (Connal et al., 2023; Pal et al., 2022).

Heterogeneity of cancer, even those having the same histologic type, complicates cancer screening. Screening tests are often performed periodically. Some cancers may be undetected initially and come clinically detectable before the next screen. Especially, more aggressive cancers fit this pattern and are missed in cancer screening. Therefore, screening tests are more sensitive to detect low grade cancers than high-grade ones (Jackson, 2008). Hence, our results with PCa are rather promising, because PSA-values used as a gold standard for PCa screening (Descotes, 2019) did not distinguish the aggressiveness of the cancer, and mCa was reliably detected from non-metastatic and non-cancerous ones. Therefore, the phage-biosensors developed herein, can be an option to improve screening of these aggressive cancer types from milder ones and for instance, could be combined with other screening tests.

Cancer detection methods often lack either analytical sensitivity or detection speed (Falkowski et al., 2021). For example, ovarian cancer biomarker HE4 was detected from urine with smartphone application and reached sensitivity and specificity of 90%. However, the method was based on ELISA which requires several incubation steps (1 hour or longer) (Wang et al., 2011). New phage-biosensors have potential to meet both requirements for sensitivity and speed (Falkowski et al., 2021). Especially, SPR-based applications have gained interest lately and for example, an ultrasensitive phage-biosensor was reported to detect carcinoembryonic antigen from serum (Hou et al., 2023). Though SPR provides high specificity and highly detailed information from molecular interactions between the target and biosensor (Kim et al., 2016), our phage-biosensor approach can be considered more universal and quite opposite to SPR.

During the development of phage-biosensors, the affinity selection was performed with whole or fractionized sample pools containing most likely more than

one cancer related biomarker. Cancer cells, and especially malignant cells in the urinary tract, leak and excrete metabolites and biomarkers to urine due to the altered metabolism (Macklin et al., 2020). Most likely biomarkers are peptides and proteins because of the hydrophilic polystyrene used in coating. An additional possibility is that cancerous samples may lack some biomarkers that non-cancerous samples contain. Therefore, the method enables development of the test without exactly knowing the target biomarkers. However, interactions between biomarkers and phage-biosensor must be characterized and the method properly validated before the clinical (Pal et al., 2022). This includes sequencing the phages, determining phage surface peptides participating the interactions, identifying the biomarkers with established methods, such as in liquid chromatography-mass spectrometry (LC-MS) and nuclear magnetic resonance (NMR) which have been used in urine biomarker analyses (Park et al., 2019; Slupsky et al., 2010). For now, the unidentified biomarkers can be considered as a limitation of this study. Identifying them is a priority of future studies. Notwithstanding, the capability of the system to detect single biomarkers was proved with model analytes.

Another limitation was relatively small sample sizes. Based on a citation classic publication from 1982, study **I** would have needed a sample size of 976 and study **III** sample size of 274 to justify the ROC-curve analyses with the reached analytical sensitivities and specificities (Hanley & McNeil, 1982). In **I** was only 6 aggressive samples from the total 96 samples and therefore, a clear unbalance between compared groups. In **III** was a total of 74 samples and the number of metastatic and non-metastatic cancer samples were even but the number of non-cancerous samples was smaller. Proper power calculations should be performed to estimate the required sample size (Schmidt et al., 2018) to confirm the results achieved herein. In addition, cross-reactivity with other cancers than PCa was not tested in **I** and cancer-specific biosensors were not developed in **III**. These aspects should be studied as a part of studies with a larger sample size.

In **III**, results from kinetic measurements were different with metastatic, non-metastatic and non-cancerous samples which proves that the interactions between samples and phage-biosensor are different. Not only did the magnitude of the slopes vary, but also the direction of the slope was positive with the metastatic sample and negative with the non-metastatic and non-cancerous sample. This may be due to differences in interactions and molecular ordering, which are likely a consequence of the well-known LC behaviour of the phages (Dogic & Fraden, 2000, 2006; Sawada, 2017; Yang et al., 2013). Because phage LCs are sensitive to external factors (Lim et al., 2019), the rationale is that the presence of metastasis biomarkers leads to a different molecular ordering compared to samples where these biomarkers are absent. Besides, the only changing factor was the sample in the measurements, and all other factors were kept the same throughout the assay.

6.4 Liquid crystalline properties of phage-biosensor

In **II**, we aimed to study the phenomena behind the detection reaction. Optical properties of the phage-biosensor were studied because self-assembly, liquid crystalline and optical properties of M13 phage are well known (Lim et al., 2019; Liu et al., 2014; Sawada, 2017; Secor et al., 2015; Yang et al., 2013). The used model analyte was bioluminescent GFP; widely used in biomedical applications (Chalfie, 1995).

We hypothesized that the detection with the phage-biosensor was based on self-assembly and LC behaviour of the phages. LC systems can be lyotropic and/or thermotropic where phage concentration or respectively temperature has an effect on the phase behaviour in the system (Liu et al., 2014; Sawada, 2017; Yang et al., 2013). The results from lyotropic and thermotropic assays (**II**) support this theory though the phage concentration and temperature had clear effects on the detection. The optimal phage concentration was different for colorimetric and TRF measurements. The biosensor had the best performance in the highest temperature (+50 °C) which can indicate faster phase transitions by enhanced thermal movement of the phages (Yang et al., 2013). Other supportive results were 1) stabilization of colour over time in colorimetric assay because after LCs are formed via supramolecular interactions, they cannot be dispersed back to aqueous form (Liu et al., 2014), 2) changes in absorbance spectrum corresponding to analyte detection; similar changes with LCs have been reported earlier by Petriashvili *et al.* (Petriashvili et al., 2009), 3) changes in the refractive index during the detection and compared to primed library; as known refractive index is an important optical parameter determining biological materials and used in many clinical applications (Khan et al., 2021), and 4) unexpectedly luminescence signal measured from GFP was enhanced when measured with GFP-specific biosensor; somehow molecular ordering possibly changes the optical environment more favourable for GFP. In addition, similar signal enhancement has been gained when M13 was genetically modified and integrated with SERS-active metal nanoparticles (Lee et al., 2014).

Despite the substantial indications of LC behaviour (optical measurements and irreversibility of the phenomenon) in the phage-biosensor system, the biophysical properties and interactions of phage-biosensor should be studied further. The interactions between target analyte and bifunctional phages should be studied in more detail with routine methods such as isothermal titration calorimetry, SPR, and electron microscopy. This would reveal the binding mechanisms between biosensor components and ensure the LC behaviour in the system. In addition, highly detailed technical description of the method is needed for clinical applicability and approval of the system since a plethora of new biomarkers and methods lack proper validation (Pal et al., 2022).

6.5 Chemical sensor

The chemical sensor used in studies **I** and **III** was a non-fluorescent dye, 7-hydroxy-3H-phenoxazin-3-one-10-oxide sodium salt, commonly known as resazurin sodium salt. It was selected based on a chemical library screen containing tens of different chemicals. Resazurin indicated reactivity with lethal PCa (GG 4–5) samples by TRF measurement (**I**) and with cancer samples measured by absorbance (**III**).

Results from **III** showed generic classification of cancerous urine samples from controls but did not distinguish more aggressive mCa from non-metastatic ones. The classification result with absorbance was not combined to other measurements but was significant when analysed alone. In publication **I**, results with resazurin improved detection of lethal PCa when measurement data was combined with biosensor results. In addition, we only measured TRF because correlation between absorbance and colour was not known at that time. Most likely absorbance measurements with a sample cohort in **I** would have revealed more information about specificity of absorbance measurement generally to cancer or aggressivity of cancer. However, the significance in **III** was so great ($p < 0.0001$) that unspecific relation to cancer in general can be justified. Also, TRF measurement yielded a significant result ($p = 0.007$) in cancer detection with resazurin, but the result was less significant in comparison. The factors behind this detection event are probably partly the same with TRF and absorbance. Resazurin is known to change colour via oxidation (Neufeld et al., 2018; O'Brien et al., 2000). Therefore, detection of cancer is most likely related to interactions between chemical sensor and metabolic products or byproducts excreted to urine. These metabolites can be directly from cancer cells or other cells affected by cancer-altered metabolism (Massagué & Ganesh, 2021; Neufeld et al., 2018).

The chemical sensor reached sensitivity and specificity 71% (95% CI 50–86%) and 75% (95% CI 62–85%) which are not yet satisfactory for cancer screening as such (**III**). However, detection was quick. Absorbance was measured already after 5 min with the chemical sensor. Therefore, this approach could bring additional value to cancer screening when combined with other methods by multiplexing (Connal et al., 2023; Pal et al., 2022).

6.6 Data analysis

Median (**I**, **III**) was used with clinical samples and mean (**II**) was used with model analytes in analysis. Mean is more sensitive for outliers than median that does not assume normally distributed data. Therefore, median was used for clinical samples that have more interfering factors than measurements with a model analyte. Three replicate measurements were used to ensure repeatability of the measurement and reveal potential flagrant outliers.

Normalization of measurement data developed throughout the studies. In **I**, measurements were not normalized but medians were calculated from raw data and used in the analysis. In **II**, signals were standardized with a blank sample and these normalized means were used in the analysis. In **III**, signals of each sample measured with the biosensor were normalized towards respective measurements with the biosensor only having affinity towards the dye. We observed that different normalization methods improved the classification power of the assays. Therefore, if the results from study **I** were reanalyzed, they might be enhanced by applying different normalizing approaches, such as normalizing the results against measurements with a blank sample (saline solution) or a control biosensor. In addition, our most recent finding was that analysis results could be improved by proportioning TRF and absorbance measurements with each other (Kulpakko & Cudjoe, 2024).

In **I** and **III**, statistical significance was estimated with unpaired t-test with Welch's correction because we did not assume the measurement data be normally distributed. Confidence intervals for sensitivity and specificity calculations were set to 95% which is commonly used within the field. In **II**, the LoD was calculated by formula (mean + 3 SD of the blank sample) commonly used for biomedical tests. Limit for statistical significance was generally used < 0.05 in all studies. Because of the high sensitivity requirements for molecular cancer diagnostics (Falkowski et al., 2021; Kumar et al., 2023; Pal et al., 2022), it could have been set even lower. However, substantially lower p-values were reached with the biosensors and chemical sensor. Linear combination was used combining measurement data from different assays in **I**. In **III**, combination of measurements was not performed and that potentially could have improved the classification results.

6.7 Clinical impact and future perspectives

Modern cancer screening and diagnostics have many requirements that current methods do not meet. New clinical diagnostics should be highly sensitive, specific, rapid, user-friendly, affordable, and minimally invasive (Chadha et al., 2022; Kaur et al., 2022; Pal et al., 2022; Peltomaa et al., 2019). Optical phage-biosensors, like one reported in this thesis, could be an alternative to overcome these challenges and create clinical impact.

Many cancers are detected only in an advanced stage because proper screening methods are lacking. The method development should focus on early detection that can have a major impact on the prognosis of the patient (Bax et al., 2019; Pal et al., 2022; Weissleder, 2006). Phage-biosensors reported in this thesis could distinguish different stages of cancer (**I**, **III**) and could be applied to early detection of cancer. The chemical sensor indicated a general detection of cancer, which could have

potential clinical value (III). However, simply classifying the most aggressive variants based on screening of urine could improve clinical cancer management (Jackson, 2008). Early detection requires discovery of new biomarkers (Weissleder, 2006) and new detection methods (Falkowski et al., 2021; Kumar et al., 2023; Pal et al., 2022).

Our phage-biosensor method offers both. A new method that brings a possibility to find new biomarkers from non-invasive liquid biopsies, such as urine. Harvesting cancer-specific biomarkers from urine samples with phages having affinity towards them is rather simple and quick. These harvested biomarkers can be identified for example with LC-MS. They can provide information from clinical cancer development and malignancy that could not only improve detection but treatment and prognosis of cancer. Non-invasive sampling is also pleasant and quick for patients, does not require special expertise (Pal et al., 2022) and is safe for personnel. Therefore, non-invasive sampling could have a clear practical impact in healthcare.

Clinical cancer screening and diagnostics would account for testing with quick detection time (Chadha et al., 2022). In addition, tests should be accurate with high analytical sensitivity and specificity. Often both requirements are not met (Falkowski et al., 2021). Based on our results and literature, phage-biosensors can meet these requirements (Kim et al., 2020) when compared to established methods (Connal et al., 2023; Kumar et al., 2023; Sekhoacha et al., 2022). The cancer in general was detected after 5 min with the chemical sensor, PCa after 2 hours and mCa after 3 hours at maximum. The biosensors do not yet meet requirements for quick testing, but their detection time could be optimized. This will require further investigation into the LC behaviour of the biosensor system, for example. In addition, attention should be given to the slope of the signal development. All in all, we have indicative results that may reveal the detection result earlier.

The phage-biosensor system has some advantages and limitations when compared to other fluorescent detection methods. It is label-free method unlike FRET; does not allow real-time monitoring of molecular interactions like SPR but provides a more holistic and multiplexed approach; and is not as sensitive and complex as SPR or SERS (Kim et al., 2016). However, from a clinical point of view, colorimetric biosensors are particularly tempting (Peltomaa et al., 2016). Colorimetric detection with the phage-biosensor system was successful partly with aggressive PCa (I) and fully with mCa (III).

An interesting aspect of our phage-biosensors is their capability to detect most likely several similar cancer-specific biomarkers at once. Results from biomarker-specific phage-biosensors can be combined and a comprehensive fingerprint from the sample and biomolecular content can be generated. This kind of semi-specificity could create clinical value because most of the methods are targeting only one biomarker at the time (Bhasin et al., 2020; Mohan et al., 2013; Pourakbari et al.,

2022; Wang et al., 2022; Zeng et al., 2022; Zhan et al., 2022). Particularly, because cancers are heterogenic by their nature which makes their reliable detection based on a single biomarker unrealistic. Therefore, multiplexed assays detecting various biomarkers simultaneously or combining results from several tests will gain attention and create clinical impact (Pal et al., 2022). In addition, a test detecting multiple cancers at once, including less prevalent ones (Connal et al., 2023), or detecting high grade cancers at early-stage (Jackson, 2008), would be clinically valuable. Our phage-biosensors could be used as a complementary method to improve existing screening and detection methods. For example, it could be used to distinguish high grade PCa or mCa alongside PSA measurements.

Finally, cost of testing is an important factor in cancer screening and diagnostics. From a health economic point of view, cancers should be detected as early as possible when they are more affordable to treat and are usually curable (Bax et al., 2019; Pal et al., 2022). Low-cost testing enables screening for a larger population which fosters public health and equality. However, the risks and harms of cancer screening should not be undervalued (Caverly et al., 2016). Anyhow, phage-biosensors provide an affordable method for cancer detection due to low production cost and easy large-scale production.

Before phage-biosensors are routinely used in clinical cancer screening and diagnostics, comprehensive validation studies must be performed. However, they have great potential to provide new biomedical detection methods fulfilling the needs of modern healthcare.

7 Conclusions

In this study, we first developed a phage-biosensor system, and then successfully tested it with a model analyte in a controlled environment. Then optical detection phenomena were characterized in detail and were most likely related to the LC behaviour of phages. Further, the method was applied to detect aggressive PCa and mCa from non-invasive urine samples. This thesis provided new knowledge from biophysical properties of phage-biosensors and their use in optical detection of biomolecules.

The following main conclusions have been drawn based on the results of our studies:

- I** Developed biopanning protocol based on affinity-selection of phages yielded bifunctional phage-biosensors targeting reporting dye molecule and target analyte. The model analyte was specifically detected, and lethal PCa was screened among clinical urine samples.
- II** Detection phenomena was most likely based on molecular ordering, phase transitions and LC behaviour of M13 phages. Results from various optical measurements provided sufficient proof to support the conclusion.
- III** The method was improved by fractionizing urine samples before affinity-selection, and normalizing measurements. mCa was accurately detected from urine with the phage-biosensors. Detection is most likely based on the metabolites excreted to urine by cancer cells, and especially mCa cells.

All in all, the phage-biosensors are a potential alternative for simple, accurate and affordable clinical detection of cancers from non-invasive urine samples. Besides, they provide an alternative for current methods to develop modern detection systems to challenging or novel matrices.

Acknowledgements

These studies were conducted as part of an industrial collaboration between the Laboratory of Biophysics, Institute of Biomedicine, University of Turku, and Aqsens Health Ltd. My doctoral studies were supported by funding from Cancer Foundation Finland sr, Southwest Finland Cancer Societys, Säästöpankki Fund, as well as travel grants from The Turku Molecular Medicine Doctoral Program (TuDMM) and People's Cultural Foundation (Kansan Sivistysrahasto).

I want to express my gratitude to my main supervisor, Professor Pekka Hänninen, who has gently but determinedly guided me in the academic world, mentoring and challenging my scientific thinking. I also had the privilege of having Chief Scientific Officer Janne Kulpakko from Aqsens as my other supervisor. Beyond being a supervisor, you are a colleague and a friend. Without you and your creative scientific insights, this dissertation would not exist, as it builds upon your extensive research in the footsteps of Pekka. Thank you for your support, trust, and appropriate challenge during my doctoral studies.

Without my employer, Aqsens Health, and their enthusiasm for phage biosensors, I would not have been able to conduct these studies. Special thanks to CEO Timo Teimonen for encouraging me to pursue this path and for fostering my development in the scientific world. My gratitude also extends to the entire Aqsens team for their support throughout my research.

As a young researcher, I have greatly benefited from the guidance of more experienced colleagues. I would like to thank Professors Mikael Skurnik and Caglar Elbuken for their valuable comments and insights on my dissertation draft as pre-examiners. I am deeply grateful for their help in refining my dissertation into a more coherent and comprehensible form. I sincerely thank my follow-up committee members, Professors Jouko Vepsäläinen, Linda Amoah, and Docent Maria Sundvall, for their care, interest, and support throughout my journey as a doctoral researcher. I am also grateful to my co-authors without whom these publications would not have seen the light of day.

During my doctoral research, I had the opportunity to visit esteemed research institutes, even though not all of that work is included in this dissertation. I would like to extend my warm thanks to the research teams at the Public Health Foundation

of India, Noguchi Memorial Institute for Medical Research, and the Laboratory of Precision and Nanomedicine at the University of Tartu, led by Professor Tambet Teesalu.

Believing in oneself requires role models and those who have achieved ambitious goals. My godmother, Marjut Lehti-Laakso, was the only PhD I knew in my childhood, and her accomplishments were both aspirational and inspirational. Now, about 25 years later, I am grateful to follow in her footsteps. I also want to acknowledge my more recent role models—my dear friends Roosa and Venla—who have motivated me by exemplifying the perseverance needed to complete their studies and dissertations in medicine. Their support and help during this journey has been invaluable.

Though I am dedicated to my studies and work, life is not solely about those pursuits. I am forever grateful for my dear friends with whom I can share the joys and sorrows of life. Heartfelt thanks and tight hugs to Tuuve, Eve, Riikka, Nikolai, Joonatan, Maiju, Tuomas, and Nalle for always being there for me.

My parents have always believed in me and supported me in all my endeavors. My mother is the most caring and warm-hearted person I know. I owe her a deep gratitude for selflessly taking care of me at my best and worst, and for caring for my daughter Sylvia during the long hours I dedicated to writing this dissertation. My father is the gentlest man I have ever met, who has loved me unconditionally throughout my life. He is never afraid to express how proud he is of me and my achievements.

In the early stages of my academic journey, I met my beloved husband, Joonas. Since that moment, I have been privileged to share my life with someone as fascinating as he is, possessing an admirable and boundless thirst for knowledge. Joonas has always believed in me, encouraging me to reach for the stars, just as I have with this dissertation. Together, we have achieved things I once thought impossible, and I am confident that even greater times and accomplishments await us. I love you deeply.

Finally, to my dearest Sylvia: Completing my doctoral studies and writing this dissertation shortly after your birth felt nearly impossible. Yet, we did it. On the day you were born, you were in my tummy during a lecture, and afterward, you accompanied me as I finished my last courses, publication and this dissertation. One of my favourite memories is from biostatistics mentoring, where we changed your diaper while discussing topics with the teacher. You have been my greatest motivation. You are the most amazing and kindest baby in the world. I cannot thank you enough or express the depth of my limitless love for you.

Home in Nummenpakka, 1.11.2024



References

- Abello, N., Kerstjens, H. A. M., Postma, D. S., & Bischoff, R. (2007). Selective acylation of primary amines in peptides and proteins. *Journal of Proteome Research*, 6(12), 4770–4776. <https://doi.org/10.1021/pr070154e>
- Ahovan, Z. A., Hashemi, A., De Plano, L. M., Gholipourmalekabadi, M., & Seifalian, A. (2020). Bacteriophage based biosensors: Trends, outcomes and challenges. In *Nanomaterials* (Vol. 10, Issue 3). MDPI AG. <https://doi.org/10.3390/nano10030501>
- Alfaleh, M. A., Alsaab, H. O., Mahmoud, A. B., Alkayyal, A. A., Jones, M. L., Mahler, S. M., & Hashem, A. M. (2020). Phage Display Derived Monoclonal Antibodies: From Bench to Bedside. In *Frontiers in Immunology* (Vol. 11). Frontiers Media S.A. <https://doi.org/10.3389/fimmu.2020.01986>
- Algar, W. R., Hildebrandt, N., Vogel, S. S., & Medintz, I. L. (2019). FRET as a biomolecular research tool — understanding its potential while avoiding pitfalls. *Nature Methods*, 16(9), 815–829. <https://doi.org/10.1038/s41592-019-0530-8>
- Ansari, G., Pal, A., Srivastava, A. K., & Verma, G. (2023). Detection of hemoglobin concentration in human blood samples using a zinc oxide nanowire and graphene layer heterostructure based refractive index biosensor. *Optics and Laser Technology*, 164. <https://doi.org/10.1016/j.optlastec.2023.109495>
- Barber, N., & Ali, A. (2022). *Urologic Cancers* (N. Barber & A. Ahmed, Eds.). Exon Publications.
- Bax, C., Lotesoriere, B. J., Sironi, S., & Capelli, L. (2019). Review and comparison of cancer biomarker trends in urine as a basis for new diagnostic pathways. In *Cancers* (Vol. 11, Issue 9). MDPI AG. <https://doi.org/10.3390/cancers11091244>
- Benchimol, S., Becker, A., Murialdo, H., & Gold, M. (1978). *The Role of the Bacteriophage XFI Gene Product during Phage Head Assembly in Vitro*.
- Bennett, N. J., Gagic, D., Sutherland-Smith, A. J., & Rakonjac, J. (2011). Characterization of a dual-function domain that mediates membrane insertion and excision of Ff filamentous bacteriophage. *Journal of Molecular Biology*, 411(5), 972–985. <https://doi.org/10.1016/j.jmb.2011.07.002>
- Bhalla, N., Jolly, P., Formisano, N., & Estrela, P. (2016). Introduction to biosensors. *Essays in Biochemistry*, 60(1), 1–8. <https://doi.org/10.1042/EBC20150001>
- Bhasin, A., Sanders, E. C., Ziegler, J. M., Briggs, J. S., Drago, N. P., Attar, A. M., Santos, A. M., True, M. Y., Ogata, A. F., Yoon, D. V., Majumdar, S., Wheat, A. J., Patterson, S. V., Weiss, G. A., & Penner, R. M. (2020). Virus Bioresistor (VBR) for Detection of Bladder Cancer Marker DJ-1 in Urine at 10 pM in One Minute. *Analytical Chemistry*, 92(9), 6654–6666. <https://doi.org/10.1021/acs.analchem.0c00534>
- Bi, L., Zhang, H., Hu, W., Chen, J., Wu, Y., Chen, H., Li, B., Zhang, Z., Choo, J., & Chen, L. (2023). Self-assembly of Au@AgNR along M13 framework: A SERS nanocarrier for bacterial detection and killing. *Biosensors and Bioelectronics*, 237. <https://doi.org/10.1016/j.bios.2023.115519>
- Bolton, J. R. (1996). Glossary of terms used in photochemistry (IUPAC Recommendations 1996). *Pure and Applied Chemistry*, 68(12), 2223–2286.

- Brödel, A. K., Isalan, M., & Jaramillo, A. (2018). Engineering of biomolecules by bacteriophage directed evolution. In *Current Opinion in Biotechnology* (Vol. 51, pp. 32–38). Elsevier Ltd. <https://doi.org/10.1016/j.copbio.2017.11.004>
- Carmody, C. M., Goddard, J. M., & Nugen, S. R. (2021). Bacteriophage Capsid Modification by Genetic and Chemical Methods. In *Bioconjugate Chemistry* (Vol. 32, Issue 3, pp. 466–481). American Chemical Society. <https://doi.org/10.1021/acs.bioconjchem.1c00018>
- Caverly, T. J., Hayward, R. A., Reamer, E., Zikmund-Fisher, B. J., Connochie, D., Heisler, M., & Fagerlin, A. (2016). Presentation of Benefits and Harms in US Cancer Screening and Prevention Guidelines: Systematic Review. In *Journal of the National Cancer Institute* (Vol. 108, Issue 6). Oxford University Press. <https://doi.org/10.1093/jnci/djv436>
- Chadha, U., Bhardwaj, P., Agarwal, R., Rawat, P., Agarwal, R., Gupta, I., Panjwani, M., Singh, S., Ahuja, C., Selvaraj, S. K., Banavoth, M., Sonar, P., Badoni, B., & Chakravorty, A. (2022). Recent progress and growth in biosensors technology: A critical review. In *Journal of Industrial and Engineering Chemistry* (Vol. 109, pp. 21–51). Korean Society of Industrial Engineering Chemistry. <https://doi.org/10.1016/j.jiec.2022.02.010>
- Chalfie, M. (1995). GREEN FLUORESCENT PROTEIN. *Photochemistry and Photobiology*, 62(4), 651–656. <https://doi.org/10.1111/j.1751-1097.1995.tb08712.x>
- Chen, C., & Wang, J. (2020). Optical biosensors: An exhaustive and comprehensive review. In *Analyst* (Vol. 145, Issue 5, pp. 1605–1628). Royal Society of Chemistry. <https://doi.org/10.1039/c9an01998g>
- Chung, W. J., Lee, D. Y., & Yoo, S. Y. (2014). Chemical modulation of m13 bacteriophage and its functional opportunities for nanomedicine. *International Journal of Nanomedicine*, 9(1), 5825–5836. <https://doi.org/10.2147/IJN.S73883>
- Cialla-May, D., Bonifacio, A., Bocklitz, T., Markin, A., Markina, N., Fornasaro, S., Dwivedi, A., Dib, T., Farnesi, E., Liu, C., Ghosh, A., & Popp, J. (2024). Biomedical SERS - the current state and future trends. In *Chemical Society Reviews*. Royal Society of Chemistry. <https://doi.org/10.1039/d4cs00090k>
- Coelho, R. W. P., Pinho, J. D., Moreno, J. S., Garbis, D. V. E. O., Do Nascimento, A. M. T., Larges, J. S., Calixto, J. R. R., Ramalho, L. N. Z., Da Silva, A. A. M., Nogueira, L. R., De Moura Feitoza, L., & Silva, G. E. B. (2018). Penile cancer in Maranhão, Northeast Brazil: The highest incidence globally? *BMC Urology*, 18(1). <https://doi.org/10.1186/s12894-018-0365-0>
- Connal, S., Cameron, J. M., Sala, A., Brennan, P. M., Palmer, D. S., Palmer, J. D., Perlow, H., & Baker, M. J. (2023). Liquid biopsies: the future of cancer early detection. In *Journal of Translational Medicine* (Vol. 21, Issue 1). BioMed Central Ltd. <https://doi.org/10.1186/s12967-023-03960-8>
- Costa, S. P., Nogueira, C. L., Cunha, A. P., Lisac, A., & Carvalho, C. M. (2023). Potential of bacteriophage proteins as recognition molecules for pathogen detection. In *Critical Reviews in Biotechnology* (Vol. 43, Issue 5, pp. 787–804). Taylor and Francis Ltd. <https://doi.org/10.1080/07388551.2022.2071671>
- DePorter, S. M., & McNaughton, B. R. (2014). Engineered M13 Bacteriophage Nanocarriers for Intracellular Delivery of Exogenous Proteins to Human Prostate Cancer Cells. *Bioconjugate Chemistry*, 25(9), 1620–1625. <https://doi.org/10.1021/bc500339k>
- Descotes, J. L. (2019). Diagnosis of prostate cancer. In *Asian Journal of Urology* (Vol. 6, Issue 2, pp. 129–136). Editorial Office of Asian Journal of Urology. <https://doi.org/10.1016/j.ajur.2018.11.007>
- Devaraj, V., Han, J., Kim, C., Kang, Y. C., & Oh, J. W. (2018). Self-assembled nanoporous biofilms from functionalized nanofibrous M13 bacteriophage. *Viruses*, 10(6). <https://doi.org/10.3390/v10060322>
- Diamandis, E. P. (1988). Immunoassays with Time-Resolved Fluorescence Spectroscopy: Principles and Applications. In *Clin Biochem* (Vol. 21).
- Dias, J., Lama, L., Gantelius, J., & Andersson-Svahn, H. (2016). Minimizing antibody cross-reactivity in multiplex detection of biomarkers in paper-based point-of-care assays. *Nanoscale*, 8(15), 8195–8201.

- Dion, M. B., Oechlin, F., & Moineau, S. (2020). Phage diversity, genomics and phylogeny. In *Nature Reviews Microbiology* (Vol. 18, Issue 3, pp. 125–138). Nature Research. <https://doi.org/10.1038/s41579-019-0311-5>
- Dogic, Z., & Fraden, S. (2000). Cholesteric phase in virus suspensions. *Langmuir*, 16(20), 7820–7824. <https://doi.org/10.1021/la000446t>
- Dogic, Z., & Fraden, S. (2006). Ordered phases of filamentous viruses. In *Current Opinion in Colloid and Interface Science* (Vol. 11, Issue 1, pp. 47–55). <https://doi.org/10.1016/j.cocis.2005.10.004>
- Du, Z., Chen, W., Xia, Q., Shi, O., & Chen, Q. (2020). Trends and projections of kidney cancer incidence at the global and national levels, 1990–2030: A Bayesian age-period-cohort modeling study. *Biomarker Research*, 8(1). <https://doi.org/10.1186/s40364-020-00195-3>
- Duong, M. M., Carmody, C. M., Ma, Q., Peters, J. E., & Nugen, S. R. (2020). Optimization of T4 phage engineering via CRISPR/Cas9. *Scientific Reports*, 10(1). <https://doi.org/10.1038/s41598-020-75426-6>
- Dy, G. W., Gore, J. L., Forouzanfar, M. H., Naghavi, M., & Fitzmaurice, C. (2017). Global Burden of Urologic Cancers, 1990–2013. In *European Urology* (Vol. 71, Issue 3, pp. 437–446). Elsevier B.V. <https://doi.org/10.1016/j.eururo.2016.10.008>
- Edgar, R., & Lielausis, I. (1968). Some steps in the assembly of bacteriophage T4. *Journal of Molecular Biology*, 32(2), 264–276.
- Elbreki, M., Ross, R. P., Hill, C., O’Mahony, J., McAuliffe, O., & Coffey, A. (2014). Bacteriophages and Their Derivatives as Biotherapeutic Agents in Disease Prevention and Treatment. *Journal of Viruses*, 2014, 1–20. <https://doi.org/10.1155/2014/382539>
- Elois, M. A., Silva, R. da, Pilati, G. V. T., Rodríguez-Lázaro, D., & Fongaro, G. (2023). Bacteriophages as Biotechnological Tools. In *Viruses* (Vol. 15, Issue 2). MDPI. <https://doi.org/10.3390/v15020349>
- Falkowski, P., Lukaszewski, Z., & Gorodkiewicz, E. (2021). Potential of surface plasmon resonance biosensors in cancer detection. In *Journal of Pharmaceutical and Biomedical Analysis* (Vol. 194). Elsevier B.V. <https://doi.org/10.1016/j.jpba.2020.113802>
- Fard, G. B., Ahmadi, M. H., Gholamin, M., Amirfakhrian, R., Saberi Teimourian, E., Karimi, M. A., & Hosseini Bafghi, M. (2024). CRISPR-Cas9 technology: As an efficient genome modification tool in the cancer diagnosis and treatment. In *Biotechnology and Bioengineering* (Vol. 121, Issue 2, pp. 472–488). John Wiley and Sons Inc. <https://doi.org/10.1002/bit.28603>
- Farwell, M. D., Pryma, D. A., & Mankoff, D. A. (2014). PET/CT imaging in cancer: Current applications and future directions. In *Cancer* (Vol. 120, Issue 22, pp. 3433–3445). John Wiley and Sons Inc. <https://doi.org/10.1002/cncr.28860>
- Feng, R., Li, G., Ko, C. N., Zhang, Z., Wan, J. B., & Zhang, Q. W. (2023). Long-Lived Second Near-Infrared Luminescent Probes: An Emerging Role in Time-Resolved Luminescence Bioimaging and Biosensing. In *Small Structures* (Vol. 4, Issue 2). John Wiley and Sons Inc. <https://doi.org/10.1002/ssr.202200131>
- Fernandes, F., Loura, L. M. S., Koehorst, R., Spruijt, R. B., Hemminga, M. A., Fedorov, A., & Prieto, M. (2004). Quantification of protein-lipid selectivity using FRET: Application to the M13 major coat protein. *Biophysical Journal*, 87(1), 344–352. <https://doi.org/10.1529/biophysj.104.040337>
- Flitcroft, J. G., Verheyen, J., Vemulkar, T., Welbourne, E. N., Rossi, S. H., Welsh, S. J., Cowburn, R. P., & Stewart, G. D. (2022). Early detection of kidney cancer using urinary proteins: a truly non-invasive strategy. In *BJU International* (Vol. 129, Issue 3, pp. 290–303). John Wiley and Sons Inc. <https://doi.org/10.1111/bju.15601>
- Gallegos, J., & Stokkermans, T. (2023). *Refractive Index*. StatPearls [Internet].
- Guttman, B., Raya, R., & Kutter, E. (2004). Basic Phage Biology. In *Bacteriophages Biology and Applications* (pp. 32–32). CRC Press.
- Haight, N. G., & Webster, R. E. (1999). *The pI and pXI Assembly Proteins Serve Separate and Essential Roles in Filamentous Phage Assembly*. <http://www.idealibrary.com>
- Hajdu, S. I. (2011). A note from history: Landmarks in history of cancer, part 1. In *Cancer* (Vol. 117, Issue 5, pp. 1097–1102). <https://doi.org/10.1002/cncr.25553>

- Hanahan, D. (2022). Hallmarks of Cancer: New Dimensions. In *Cancer Discovery* (Vol. 12, Issue 1, pp. 31–46). American Association for Cancer Research Inc. <https://doi.org/10.1158/2159-8290.CD-21-1059>
- Hanahan, D., & Weinberg, R. A. (2000). The Hallmarks of Cancer Review evolve progressively from normalcy via a series of pre. In *Cell* (Vol. 100).
- Hanahan, D., & Weinberg, R. A. (2011). Hallmarks of cancer: The next generation. In *Cell* (Vol. 144, Issue 5, pp. 646–674). <https://doi.org/10.1016/j.cell.2011.02.013>
- Hanley, J. A., & McNeil, B. J. (1982). The Meaning and Use of the Area under a Receiver Operating Characteristic (ROC) Curve. *Diagnostic Radiology*, *143*(1), 29–36.
- Hay, I. D., & Lithgow, T. (2019). Filamentous phages: masters of a microbial sharing economy. *EMBO Reports*, *20*(6). <https://doi.org/10.15252/embr.201847427>
- Hosseini, S., Marco, P. V.-V., Sergio, R.-P., & Martinez-Chapa, O. (2018). *Enzyme-linked Immunosorbent Assay (ELISA) From A to Z*. Springer Briefs in Applied Sciences and Technology. <https://doi.org/https://doi.org/10.1007/978-981-10-6766-2>
- Hou, J., Xu, Y., Sun, S., Zhong, X., Yang, C. T., & Zhou, X. (2023). Gold nanoparticles-decorated M13 phage SPR probe for dual detection of antigen biomarkers in serum. *Sensors and Actuators B: Chemical*, *374*. <https://doi.org/10.1016/j.snb.2022.132811>
- Huang, J., Chan, S. C., Tin, M. S., Liu, X., Lok, V. T. T., Ngai, C. H., Zhang, L., Lucero-Prisno, D. E., Xu, W., Zheng, Z. J., Chiu, P. K. F., Ng, A. C. F., Enikeev, D., Nicol, D., Spiess, P. E., Laguna, P., Teoh, J. Y. C., & Wong, M. C. S. (2022). Worldwide Distribution, Risk Factors, and Temporal Trends of Testicular Cancer Incidence and Mortality: A Global Analysis. *European Urology Oncology*, *5*(5), 566–576. <https://doi.org/10.1016/j.euo.2022.06.009>
- Jackson, B. R. (2008). The Dangers of False-Positive and False-Negative Test Results: False-Positive Results as a Function of Pretest Probability. In *Clinics in Laboratory Medicine* (Vol. 28, Issue 2, pp. 305–319). <https://doi.org/10.1016/j.cll.2007.12.009>
- Kamel, S., & Khattab, T. A. (2020). Recent advances in cellulose-based biosensors for medical diagnosis. In *Biosensors* (Vol. 10, Issue 6). MDPI. <https://doi.org/10.3390/BIOS10060067>
- Karoonuthaisiri, N., Charlermroj, R., Morton, M. J., Oplatowska-Stachowiak, M., Grant, I. R., & Elliott, C. T. (2014). Development of a M13 bacteriophage-based SPR detection using Salmonella as a case study. *Sensors and Actuators, B: Chemical*, *190*, 214–220. <https://doi.org/10.1016/j.snb.2013.08.068>
- Kaur, B., Kumar, S., & Kaushik, B. K. (2022). Recent advancements in optical biosensors for cancer detection. In *Biosensors and Bioelectronics* (Vol. 197). Elsevier Ltd. <https://doi.org/10.1016/j.bios.2021.113805>
- Khalil, A., Ferrer, J., Brau, R., Kottmann, S., Noren, C., Lang, M., & Belcher, A. (2007). Single M13 bacteriophage tethering and stretching. *PNAS*, *104*(12), 4892–4897. www.pnas.org/cgi/doi/10.1073/pnas.0605727104
- Khan, M., Islam, Md. K., Rahman, M., Dhondt, B., Quintero, I., Puhka, M., Jaakkola, P. M., Lamminmäki, U., & Leivo, J. (2024). Tetraspanin immunoassay for the detection of extracellular vesicles and renal cell carcinoma. *Nano Select*. <https://doi.org/10.1002/nano.202400018>
- Khan, R., Gul, B., Khan, S., Nisar, H., & Ahmad, I. (2021). Refractive index of biological tissues: Review, measurement techniques, and applications. In *Photodiagnosis and Photodynamic Therapy* (Vol. 33). Elsevier B.V. <https://doi.org/10.1016/j.pdpdt.2021.102192>
- Kim, C., Lee, H., Devaraj, V., Kim, W. G., Lee, Y., Kim, Y., Jeong, N. N., Choi, E. J., Baek, S. H., Han, D. W., Sun, H., & Oh, J. W. (2020). Hierarchical cluster analysis of medical chemicals detected by a bacteriophage-based colorimetric sensor array. *Nanomaterials*, *10*(1). <https://doi.org/10.3390/nano10010121>
- Kim, I., Moon, J. S., & Oh, J. W. (2016). Recent advances in M13 bacteriophage-based optical sensing applications. In *Nano Convergence* (Vol. 3, Issue 1). Korea Nano Technology Research Society. <https://doi.org/10.1186/s40580-016-0087-5>

- Kim, K. P., Cha, J. D., Jang, E. H., Klumpp, J., Hagens, S., Hardt, W. D., Lee, K. Y., & Loessner, M. J. (2008). PEGylation of bacteriophages increases blood circulation time and reduces T-helper type 1 immune response. *Microbial Biotechnology*, *1*(3), 247–257. <https://doi.org/10.1111/j.1751-7915.2008.00028.x>
- Kim, S. J., Lee, Y., Choi, E. J., Lee, J. M., Kim, K. H., & Oh, J. W. (2023). The development progress of multi-array colourimetric sensors based on the M13 bacteriophage. In *Nano Convergence* (Vol. 10, Issue 1). Korea Nano Technology Research Society. <https://doi.org/10.1186/s40580-022-00351-5>
- Kim, W. G., Song, H., Kim, C., Moon, J. S., Kim, K., Lee, S. W., & Oh, J. W. (2016). Biomimetic self-templating optical structures fabricated by genetically engineered M13 bacteriophage. *Biosensors and Bioelectronics*, *85*, 853–859. <https://doi.org/10.1016/j.bios.2016.05.099>
- Kinoshita, S., & Yoshioka, S. (2005). Structural colors in nature: The role of regularity and irregularity in the structure. In *ChemPhysChem* (Vol. 6, Issue 8, pp. 1442–1459). Wiley-VCH Verlag. <https://doi.org/10.1002/cphc.200500007>
- Kiro, R., Shitrit, D., & Qimron, U. (2014). Efficient engineering of a bacteriophage genome using the type I-E CRISPR-Cas system. *RNA Biology*, *11*(1), 42–44. <https://doi.org/10.4161/rna.27766>
- Konings, R. N. H., Hulsebos, T., & Van Den Hondel, C. A. (1975). Identification and Characterization of the In Vitro Synthesized Gene Products of Bacteriophage M13. In *JOURNAL OF VIROLOGY* (Vol. 15, Issue 3). <https://journals.asm.org/journal/jvi>
- Kulpakko, J., & Cudjoe, E. (2024, May 6th). *Oral communication*.
- Kulpakko, J., Rantakokko-Jalava, K., Eerola, E., & Hänninen, P. E. (2019). Rapid time-resolved luminescence based screening of bacteria in urine with luminescence modulating biosensing phages. *Analytical Biochemistry*, *570*, 21–26. <https://doi.org/10.1016/j.ab.2019.01.011>
- Kumar, R. R., Kumar, A., Chuang, C. H., & Shaikh, M. O. (2023). Recent Advances and Emerging Trends in Cancer Biomarker Detection Technologies. In *Industrial and Engineering Chemistry Research* (Vol. 62, Issue 14, pp. 5691–5713). American Chemical Society. <https://doi.org/10.1021/acs.iecr.2c04097>
- Lakowicz, J. R. (2006). *Principles of Fluorescence Spectroscopy Third Edition*.
- Lee, J. H., Xu, P. F., Domaille, D. W., Choi, C., Jin, S., & Cha, J. N. (2014). M13 bacteriophage as materials for amplified surface enhanced raman scattering protein sensing. *Advanced Functional Materials*, *24*(14), 2079–2084. <https://doi.org/10.1002/adfm.201303331>
- Lee, J. M., Lee, Y., Devaraj, V., Nguyen, T. M., Kim, Y. J., Kim, Y. H., Kim, C., Choi, E. J., Han, D. W., & Oh, J. W. (2021). Investigation of colorimetric biosensor array based on programable surface chemistry of M13 bacteriophage towards artificial nose for volatile organic compound detection: From basic properties of the biosensor to practical application. *Biosensors and Bioelectronics*, *188*. <https://doi.org/10.1016/j.bios.2021.113339>
- Li, Y., Bao, Q., Yang, S., Yang, M., & Mao, C. (2022). Bionanoparticles in cancer imaging, diagnosis, and treatment. In *VIEW* (Vol. 3, Issue 4). John Wiley and Sons Inc. <https://doi.org/10.1002/VIW.20200027>
- Lim, C., Ko, J., Jeon, D., Song, Y., Park, J., Ryu, J., & Lee, D. W. (2019). Probing molecular mechanisms of M13 bacteriophage adhesion. *Communications Chemistry*, *2*(1). <https://doi.org/10.1038/s42004-019-0198-0>
- Liu, K., Chen, D., Marcozzi, A., Zheng, L., Su, J., Pesce, D., Zajaczkowski, W., Kolbe, A., Pisula, W., Müllen, K., Clark, N. A., & Herrmann, A. (2014). Thermotropic liquid crystals from biomacromolecules. *Proceedings of the National Academy of Sciences of the United States of America*, *111*(52), 18596–18600. <https://doi.org/10.1073/pnas.1421257111>
- Macklin, A., Khan, S., & Kislinger, T. (2020). Recent advances in mass spectrometry based clinical proteomics: Applications to cancer research. In *Clinical Proteomics* (Vol. 17, Issue 1). BioMed Central Ltd. <https://doi.org/10.1186/s12014-020-09283-w>
- Marciano, D. K., Russel, M., & Simon, S. M. (1999). An Aqueous Channel for Filamentous Phage Export. *Science*, *284*(5419), 1516–1519.

- Marino, S. M., & Gladyshev, V. N. (2010). Cysteine Function Governs Its Conservation and Degeneration and Restricts Its Utilization on Protein Surfaces. *Journal of Molecular Biology*, 404(5), 902–916. <https://doi.org/10.1016/j.jmb.2010.09.027>
- Massagué, J., & Ganesh, K. (2021). Metastasis-initiating cells and ecosystems. In *Cancer Discovery* (Vol. 11, Issue 4, pp. 971–994). American Association for Cancer Research Inc. <https://doi.org/10.1158/2159-8290.CD-21-0010>
- Mohan, K., Donavan, K. C., Arter, J. A., Penner, R. M., & Weiss, G. A. (2013). Sub-nanomolar detection of prostate-specific membrane antigen in synthetic urine by synergistic, dual-ligand phage. *Journal of the American Chemical Society*, 135(20), 7761–7767. <https://doi.org/10.1021/ja4028082>
- Mohan, K., & Weiss, G. A. (2015). Engineering chemically modified viruses for prostate cancer cell recognition. *Molecular BioSystems*, 11(12), 3264–3272. <https://doi.org/10.1039/c5mb00511f>
- Møller-Olsen, C., Dhanoa, G., Fehér, T., & Sagona, A. (2022). Advances in engineering of bacteriophages for therapeutic applications. In V. Singh (Ed.), *New Frontiers and Applications of Synthetic Biology* (pp. 217–218). Academic Press.
- Moon, J. S., Park, M., Kim, W. G., Kim, C., Hwang, J., Seol, D., Kim, C. S., Sohn, J. R., Chung, H., & Oh, J. W. (2017). M-13 bacteriophage based structural color sensor for detecting antibiotics. *Sensors and Actuators, B: Chemical*, 240, 757–762. <https://doi.org/10.1016/j.snb.2016.09.050>
- Naresh, V., & Lee, N. (2021). A review on biosensors and recent development of nanostructured materials-enabled biosensors. In *Sensors (Switzerland)* (Vol. 21, Issue 4, pp. 1–35). MDPI AG. <https://doi.org/10.3390/s21041109>
- Netto, G. J., Amin, M. B., Berney, D. M., Compérat, E. M., Gill, A. J., Hartmann, A., Menon, S., Raspollini, M. R., Rubin, M. A., Srigley, J. R., Hoon Tan, P., Tickoo, S. K., Tsuzuki, T., Turajlic, S., Cree, I., & Moch, H. (2022). The 2022 World Health Organization Classification of Tumors of the Urinary System and Male Genital Organs—Part B: Prostate and Urinary Tract Tumors. In *European Urology* (Vol. 82, Issue 5, pp. 469–482). Elsevier B.V. <https://doi.org/10.1016/j.eururo.2022.07.002>
- Neufeld, B. H., Tapia, J. B., Lutzke, A., & Reynolds, M. M. (2018). Small Molecule Interferences in Resazurin and MTT-Based Metabolic Assays in the Absence of Cells. *Analytical Chemistry*, 90(11), 6867–6876. <https://doi.org/10.1021/acs.analchem.8b01043>
- Nguyen, T. N., Chung, J. H., Bak, G.-H., Kim, Y. H., Kim, M., Kim, Y.-J., Kwon, R. J., Choi, E.-J., Kim, K. H., Kim, S. Y., & Oh, J.-W. (2023). Multiaarray Biosensor for Diagnosing Lung Cancer Based on Gap Plasmonic Color Films. *ACS Sensors*, 8, 167–175.
- O'Brien, J., Wilson, I., Orton, T., & Pognan, F. (2000). Investigation of the Alamar Blue (resazurin) fluorescent dye for the assessment of mammalian cell cytotoxicity. *European Journal of Biochemistry*, 267(17), 5421–5426. <https://doi.org/10.1046/j.1432-1327.2000.01606.x>
- Onsager, L. (1949). THE EFFECTS OF SHAPE ON THE INTERACTION OF COLLOIDAL PARTICLES. *Molecular Interaction*, 51(4), 627–659.
- Pal, M., Muinao, T., Boruah, H. P. D., & Mahindroo, N. (2022). Current advances in prognostic and diagnostic biomarkers for solid cancers: Detection techniques and future challenges. In *Biomedicine and Pharmacotherapy* (Vol. 146). Elsevier Masson s.r.l. <https://doi.org/10.1016/j.biopha.2021.112488>
- Park, J., Shin, Y., Kim, T. H., Kim, D.-H., & Lee, A. (2019). Urinary Metabolites as Biomarkers for Diagnosis of Breast Cancer: A Preliminary Study. *Journal of Breast Disease*, 7(2), 44–51. <https://doi.org/10.14449/jbd.2019.7.2.44>
- Parkes, A., Kemm, F., He, L., & Killelea, T. (2021). CRISPR_systems_what's_new_where_next. *The Biochemist*, 43, 1–5. https://doi.org/10.1042/bio_2021_194
- Parvin, T., Ahmed, K., Alatwi, A. M., & Rashed, A. N. Z. (2021). Differential optical absorption spectroscopy-based refractive index sensor for cancer cell detection. *Optical Review*, 28(1), 134–143. <https://doi.org/10.1007/s10043-021-00644-w>

- Patrikidou, A., Cazzaniga, W., Berney, D., Boormans, J., de Angst, I., Di Nardo, D., Fankhauser, C., Fischer, S., Gravina, C., Gremmels, H., Heidenreich, A., Janisch, F., Leão, R., Nicolai, N., Oing, C., Oldenburg, J., Shepherd, R., Tandstad, T., & Nicol, D. (2023). European Association of Urology Guidelines on Testicular Cancer: 2023 Update. In *European Urology* (Vol. 84, Issue 3, pp. 289–301). Elsevier B.V. <https://doi.org/10.1016/j.eururo.2023.04.010>
- Peltomaa, R., Benito-Peña, E., Barderas, R., & Moreno-Bondi, M. C. (2019). Phage display in the quest for new selective recognition elements for biosensors. In *ACS Omega* (Vol. 4, Issue 7, pp. 11569–11580). American Chemical Society. <https://doi.org/10.1021/acsomega.9b01206>
- Peltomaa, R., López-Perolio, I., Benito-Peña, E., Barderas, R., & Moreno-Bondi, M. C. (2016). Application of bacteriophages in sensor development. In *Analytical and Bioanalytical Chemistry* (Vol. 408, Issue 7, pp. 1805–1828). Springer Verlag. <https://doi.org/10.1007/s00216-015-9087-2>
- Petrenko, V. A. (2018). Landscape phage: Evolution from phage display to nanobiotechnology. In *Viruses* (Vol. 10, Issue 6). MDPI AG. <https://doi.org/10.3390/v10060311>
- Petriashvili, G., Chanishvili, A., Chilaya, G., Matranga, M. A., De Santo, M. P., & Barberi, R. (2009). Novel UV sensor based on a liquid crystalline mixture containing a photoluminescent dye. *Molecular Crystals and Liquid Crystals, 500*, 82–90. <https://doi.org/10.1080/15421400802713736>
- Pourakbari, R., Yousefi, M., Khalilzadeh, B., Irani-nezhad, M. H., Khataee, A., Aghebati-Maleki, L., Soleimani, A., Kamrani, A., Chakari-Khiavi, F., Abolhasan, R., Motallebnezhad, M., Jadidi-Niaragh, F., Yousefi, B., Kafil, H. S., Hojjat-Farsangi, M., & Rashidi, M. R. (2022). Early stage evaluation of colon cancer using tungsten disulfide quantum dots and bacteriophage nanobiocomposite as an efficient electrochemical platform. *Cancer Nanotechnology, 13*(1). <https://doi.org/10.1186/s12645-022-00113-2>
- Rakonjac, J., Gold, V. A. M., León-Quezada, R. I., & Davenport, C. H. (2023). Structure, Biology, and Applications of Filamentous Bacteriophages. *Cold Spring Harbor Protocols*. <https://doi.org/10.1101/pdb.over107754>
- Russel, M. (1993). Protein protein interactions. *Journal of Molecular Biology, 231*(3), 689–697.
- Ryu, W.-S. (2017). Virus Life Cycle. In *Molecular Virology of Human Pathogenic Viruses* (pp. 31–45). Elsevier. <https://doi.org/10.1016/b978-0-12-800838-6.00003-5>
- Sandman, K. E., Banner, J. S., & Noren, C. J. (2000). Phage display of selenopeptides [6]. In *Journal of the American Chemical Society* (Vol. 122, Issue 5, pp. 960–961). <https://doi.org/10.1021/ja992462m>
- Savory, J., Pu, P., & Sunderman, W. (1968). A Biuret Method for Determination of Protein in Normal Urine. *Clinical Chemistry, 14*(12), 1160–1171.
- Sawada, T. (2017). Filamentous virus-based soft materials based on controlled assembly through liquid crystalline formation. In *Polymer Journal* (Vol. 49, Issue 9, pp. 639–647). Nature Publishing Group. <https://doi.org/10.1038/pj.2017.35>
- Sawada, T., & Serizawa, T. (2018). Filamentous viruses as building blocks for hierarchical self-assembly toward functional soft materials. In *Bulletin of the Chemical Society of Japan* (Vol. 91, Issue 3, pp. 455–466). Chemical Society of Japan. <https://doi.org/10.1246/bcsj.20170428>
- Schmidt, S. A. J., Lo, S., & Hollestein, L. M. (2018). Research Techniques Made Simple: Sample Size Estimation and Power Calculation. In *Journal of Investigative Dermatology* (Vol. 138, Issue 8, pp. 1678–1682). Elsevier B.V. <https://doi.org/10.1016/j.jid.2018.06.165>
- Scott, J., & Smith, G. (1990). Searching for Peptide Ligands with an Epitope Library. *Science (New York, N.Y.), 249*(4967), 386–390.
- Secor, P. R., Sweere, J. M., Michaels, L. A., Malkovskiy, A. V., Lazzareschi, D., Katznelson, E., Rajadas, J., Birnbaum, M. E., Arrigoni, A., Braun, K. R., Evanko, S. P., Stevens, D. A., Kaminsky, W., Singh, P. K., Parks, W. C., & Bollyky, P. L. (2015). Filamentous bacteriophage promote biofilm assembly and function. *Cell Host and Microbe, 18*(5), 549–559. <https://doi.org/10.1016/j.chom.2015.10.013>

- Sekhoacha, M., Riet, K., Motloung, P., Gumenku, L., Adegoke, A., & Mashele, S. (2022). Prostate Cancer Review: Genetics, Diagnosis, Treatment Options, and Alternative Approaches. In *Molecules* (Vol. 27, Issue 17). MDPI. <https://doi.org/10.3390/molecules27175730>
- Seyfried, T. N., & Huysentruyt, L. C. (2013). *On the Origin of Cancer Metastasis*.
- Shin, J. H., Yang, H. J., Kim, J. H., Yang, J. C., Park, J., & Park, J. P. (2023). Quantitative Label-free Determination of Thrombin Using a Chemically-modified M13 Virus-electrode Interface. *Biotechnology and Bioprocess Engineering*, 28(2), 235–245. <https://doi.org/10.1007/s12257-022-0361-9>
- Siegel, R. L., Miller, K. D., & Jemal, A. (2018). Cancer statistics, 2018. *CA: A Cancer Journal for Clinicians*, 68(1), 7–30. <https://doi.org/10.3322/caac.21442>
- Singh, A., Poshtiban, S., & Evoy, S. (2013). Recent advances in bacteriophage based biosensors for food-borne pathogen detection. In *Sensors (Switzerland)* (Vol. 13, Issue 2, pp. 1763–1786). <https://doi.org/10.3390/s130201763>
- Slupsky, C. M., Steed, H., Wells, T. H., Dabbs, K., Schepansky, A., Capstick, V., Faught, W., & Sawyer, M. B. (2010). Urine metabolite analysis offers potential early diagnosis of ovarian and breast cancers. *Clinical Cancer Research*, 16(23), 5835–5841. <https://doi.org/10.1158/1078-0432.CCR-10-1434>
- Smeal, S. W., Schmitt, M. A., Pereira, R. R., Prasad, A., & Fisk, J. D. (2017). Simulation of the M13 life cycle I: Assembly of a genetically-structured deterministic chemical kinetic simulation. *Virology*, 500, 259–274. <https://doi.org/10.1016/j.virol.2016.08.017>
- Smith, G. P. (1985). Filamentous Fusion Phage: Novel Expression Vectors That Display Cloned Antigens on the Virion Surface. *Science (New York, N.Y.)*, 228(4705), 1315–1317.
- Smith, G. R. (1988). Homologous Recombination in Procaryotes. In *MICROBIOLOGICAL REVIEWS* (Vol. 52, Issue 1). <https://journals.asm.org/journal/mr>
- Socher, E., & Imperiali, B. (2013). FRET-Capture: A Sensitive Method for the Detection of Dynamic Protein Interactions. *ChemBioChem*, 14(1), 53–57. <https://doi.org/10.1002/cbic.201200700>
- Sproston, N. R., & Ashworth, J. J. (2018). Role of C-reactive protein at sites of inflammation and infection. In *Frontiers in Immunology* (Vol. 9, Issue APR). Frontiers Media S.A. <https://doi.org/10.3389/fimmu.2018.00754>
- Stabile, A., Giganti, F., Rosenkrantz, A. B., Taneja, S. S., Villeirs, G., Gill, I. S., Allen, C., Emberton, M., Moore, C. M., & Kasivisvanathan, V. (2020). Multiparametric MRI for prostate cancer diagnosis: current status and future directions. In *Nature Reviews Urology* (Vol. 17, Issue 1, pp. 41–61). Nature Research. <https://doi.org/10.1038/s41585-019-0212-4>
- Suan Ng, S., Ling Lee, H., Bothi Raja, P., & Doong, R. an. (2022). Recent Advances in Nanomaterial-based Optical Biosensors as Potential Point-of-Care Testing (PoCT) Probes in Carcinoembryonic Antigen Detection. In *Chemistry - An Asian Journal* (Vol. 17, Issue 14). John Wiley and Sons Ltd. <https://doi.org/10.1002/asia.202200287>
- Takiwaki, H., Miyaoka, Y., & Arase, S. (2004). Analysis of the absorbance spectra of skin lesions as a helpful tool for detection of major pathophysiological changes. *Skin Research & Technology*, 10(2), 130–135.
- Thomas, A., Necchi, A., Muneer, A., Tobias-Machado, M., Tran, A. T. H., Van Rompuy, A. S., Spiess, P. E., & Albersen, M. (2021). Penile cancer. In *Nature Reviews Disease Primers* (Vol. 7, Issue 1). Nature Research. <https://doi.org/10.1038/s41572-021-00246-5>
- Turner, D., Shkoporov, A. N., Lood, C., Millard, A. D., Dutilh, B. E., Alfenas-Zerbini, P., van Zyl, L. J., Aziz, R. K., Oksanen, H. M., Poranen, M. M., Kropinski, A. M., Barylski, J., Brister, J. R., Chanisvili, N., Edwards, R. A., Enault, F., Gillis, A., Knezevic, P., Krupovic, M., ... Adriaenssens, E. M. (2023). Abolishment of morphology-based taxa and change to binomial species names: 2022 taxonomy update of the ICTV bacterial viruses subcommittee. *Archives of Virology*, 168(2). <https://doi.org/10.1007/s00705-022-05694-2>
- Ugai, T., Sasamoto, N., Lee, H. Y., Ando, M., Song, M., Tamimi, R. M., Kawachi, I., Campbell, P. T., Giovannucci, E. L., Weiderpass, E., Rebbeck, T. R., & Ogino, S. (2022). Is early-onset cancer an

- emerging global epidemic? Current evidence and future implications. In *Nature Reviews Clinical Oncology* (Vol. 19, Issue 10, pp. 656–673). Springer Nature. <https://doi.org/10.1038/s41571-022-00672-8>
- Valencia-Toxqui, G., & Ramsey, J. (2024). How to introduce a new bacteriophage on the block: a short guide to phage classification. *Journal of Virology*, *98*(10). <https://doi.org/10.1128/jvi.01821-23>
- Wang, H., Wang, H., Zhang, H., Huang, Y., Zhang, N., Li, W., Qiu, X., Yu, D., & Zhang, L. (2022). Integration of a multichannel surface plasmon resonance sensor chip and refractive index matching film array for protein detection in human urine. *Talanta*, *246*. <https://doi.org/10.1016/j.talanta.2022.123533>
- Wang, L., Lu, B., He, M., Wang, Y., Wang, Z., & Du, L. (2022). Prostate Cancer Incidence and Mortality: Global Status and Temporal Trends in 89 Countries From 2000 to 2019. *Frontiers in Public Health*, *10*. <https://doi.org/10.3389/fpubh.2022.811044>
- Wang, M., Zheng, Z., Zhang, Y., Wang, G., Liu, J., Yu, H., & Liu, A. (2022). An ultrasensitive label-free electrochemical impedimetric immunosensor for vascular endothelial growth factor based on specific phage via negative pre-screening. *Analytica Chimica Acta*, *1225*. <https://doi.org/10.1016/j.aca.2022.340250>
- Wang, R., Li, H. Da, Cao, Y., Wang, Z. Y., Yang, T., & Wang, J. H. (2023). M13 phage: a versatile building block for a highly specific analysis platform. In *Analytical and Bioanalytical Chemistry* (Vol. 415, Issue 18, pp. 3927–3944). Springer Science and Business Media Deutschland GmbH. <https://doi.org/10.1007/s00216-023-04606-w>
- Wang, S., Zhao, X., Khimji, I., Akbas, R., Qiu, W., Edwards, D., Cramer, D. W., Ye, B., & Demirci, U. (2011). Integration of cell phone imaging with microchip ELISA to detect ovarian cancer HE4 biomarker in urine at the point-of-care. *Lab on a Chip*, *11*(20), 3411–3418. <https://doi.org/10.1039/c1lc20479c>
- Wang, X. Y., Yang, J. Y., Wang, Y. T., Zhang, H. C., Chen, M. L., Yang, T., & Wang, J. H. (2021). M13 phage-based nanoprobe for SERS detection and inactivation of *Staphylococcus aureus*. *Talanta*, *221*. <https://doi.org/10.1016/j.talanta.2020.121668>
- Weissleder, R. (2006). Use of genomic signatures in therapeutics development in oncology and other diseases. *Pharmacogenomics Journal*, *6*(3), 166–173. <https://doi.org/10.1038/sj.tpj.6500349>
- Welch, D. R., & Hurst, D. R. (2019). Defining the Hallmarks of Metastasis. In *Cancer Research* (Vol. 79, Issue 12, pp. 3011–3027). American Association for Cancer Research Inc. <https://doi.org/10.1158/0008-5472.CAN-19-0458>
- Wezenbeek, P. M. G. F., Hulsebos, T. J. M., & Schoenmakers, J. (1980). Nucleotide sequence of the filamentous bacteriophage M13 DNA genome- comparison with phage fd. *Gene*, *11*, 129–148.
- Wilkinson, A. N. (n.d.). *Cancer diagnosis in primary care Six steps to reducing the diagnostic interval*. www.thrombosiscanada.ca.
- World Health Organization. (2024a, February 1). *Global cancer burden growing, amidst mounting need for services*.
- World Health Organization. (2024b, June 20). *Cancer today*.
- World Health Organization. (2024c, August 23). *Cancer statistics 2022*.
- Wu, J., Mayer, A. T., & Li, R. (2022). Integrated imaging and molecular analysis to decipher tumor microenvironment in the era of immunotherapy. In *Seminars in Cancer Biology* (Vol. 84, pp. 310–328). Academic Press. <https://doi.org/10.1016/j.semcancer.2020.12.005>
- Xu, L., Chopdat, R., Li, D., & Al-Jamal, K. T. (2020). Development of a simple, sensitive and selective colorimetric aptasensor for the detection of cancer-derived exosomes. *Biosensors and Bioelectronics*, *169*. <https://doi.org/10.1016/j.bios.2020.112576>
- Yang, S. H., Chung, W. J., McFarland, S., & Lee, S. W. (2013). Assembly of bacteriophage into functional materials. *Chemical Record*, *13*(1), 43–59. <https://doi.org/10.1002/tcr.201200012>
- Yaxley, J. (2016). Urinary tract cancers: An overview for general practice. *Journal of Family Medicine and Primary Care*, *5*(3), 533. <https://doi.org/10.4103/2249-4863.197258>

- Young, R., Wang, I.-N., & Roof, W. (2000). Phages will out- strategies of host cell lysis. *Trends in Microbiology*, 8(3), 120–128.
- Zeng, Y., Yue, H., Cao, B., Li, Y., Yang, M., & Mao, C. (2022). Target-Triggered Formation of Artificial Enzymes on Filamentous Phage for Ultrasensitive Direct Detection of Circulating miRNA Biomarkers in Clinical Samples. *Angewandte Chemie - International Edition*, 61(45). <https://doi.org/10.1002/anie.202210121>
- Zhan, S., Fang, H., Chen, Q., Xiong, S., Guo, Y., Huang, T., Li, X., Leng, Y., Huang, X., & Xiong, Y. (2022). M13 bacteriophage as biometric component for orderly assembly of dynamic light scattering immunosensor. *Biosensors and Bioelectronics*, 217. <https://doi.org/10.1016/j.bios.2022.114693>



**TURUN
YLIOPISTO**
UNIVERSITY
OF TURKU

ISBN 978-952-02-0009-1 (PRINT)
ISBN 978-952-02-0010-7 (PDF)
ISSN 0355-9483 (Print)
ISSN 2343-3213 (Online)

